Accepted Manuscript

Design, synthesis and biological evaluation of novel thiazolidinedione derivatives as irreversible allosteric IKK-β modulators

Ahmed Elkamhawy, Nam youn Kim, Ahmed H.E. Hassan, Jung-eun Park, Jeong-Eun Yang, Kwang-Seok Oh, Byung Ho Lee, Mi Young Lee, Kye Jung Shin, Kyung-Tae Lee, Wooyoung Hur, Eun Joo Roh

PII: S0223-5234(18)30678-0

DOI: 10.1016/j.ejmech.2018.08.020

Reference: EJMECH 10631

To appear in: *European Journal of Medicinal Chemistry*

Received Date: 24 October 2017

Revised Date: 6 August 2018

Accepted Date: 6 August 2018

Please cite this article as: A. Elkamhawy, N.y. Kim, A.H.E. Hassan, J.-e. Park, J.-E. Yang, K.-S. Oh, B.H. Lee, M.Y. Lee, K.J. Shin, K.-T. Lee, W. Hur, E.J. Roh, Design, synthesis and biological evaluation of novel thiazolidinedione derivatives as irreversible allosteric IKK-β modulators, *European Journal of Medicinal Chemistry* (2018), doi: 10.1016/j.ejmech.2018.08.020.

Graphical Abstract:

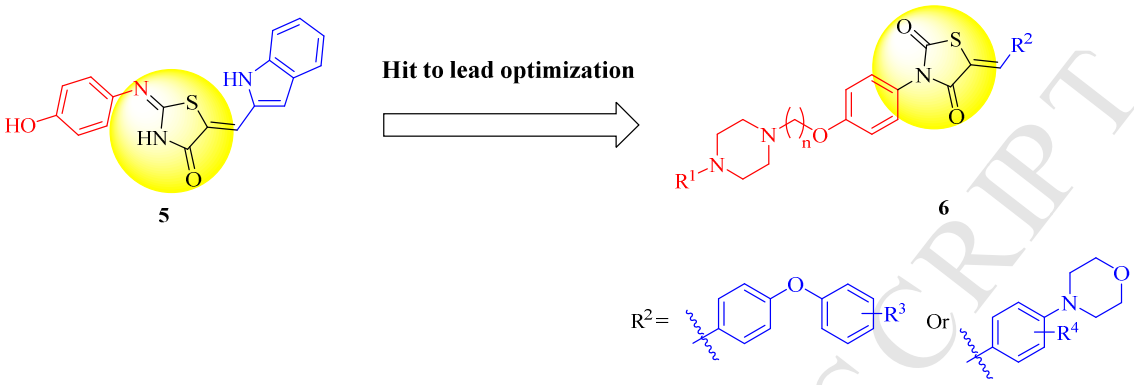

Design, synthesis and biological evaluation of novel thiazolidinedione derivatives as irreversible allosteric IKK-β modulators

Ahmed Elkamhawy[a,b,1,*], Nam youn Kim[a,1], Ahmed H.E. Hassan[c], Jung-eun Park[a], Jeong-Eun Yang[a], Kwang-Seok Oh[d], Byung Ho Lee[d], Mi Young Lee[d], Kye Jung Shin[e], Kyung-Tae Lee[f], Wooyoung Hur[a,g], Eun Joo Roh[a,g*]

[a] *Chemical Kinomics Research Center, Korea Institute of Science and Technology (KIST), Seoul 02792, Republic of Korea.*

[b] *Department of Pharmaceutical Organic Chemistry, Faculty of Pharmacy, Mansoura University, Mansoura 35516, Egypt*

[c] *Department of Medicinal Chemistry, Faculty of Pharmacy, Mansoura University, Mansoura 35516, Egypt*

[d] *Therapeutics & Biotechnology Division, Korea Research Institute of Chemical Technology, 141 Gajeong-ro, Yuseong, Daejeon 34114, Republic of Korea*

[e] *Integrated Research Institute of Pharmaceutical Sciences, College of Pharmacy, The Catholic University of Korea, Bucheon-si, Gyeonggi-do 14662, Republic of Korea.*

[f] *Department of Life and Nanopharmaceutical Sciences, Kyung Hee University, Seoul 02447, Republic of Korea.*

[g] *Division of Bio-Medical Science & Technology, KIST School, Korea University of Science and Technology, Seoul 02792, Republic of Korea*

[1] Both authors contributed equally to this work

[*] Corresponding authors:

Ahmed Elkamhawy: a_elkamhawy@mans.edu.eg; a.elkamhawy@gmail.com

Eun Joo Roh: r8636@kist.re.kr

Abstract

The kinase known as IKK-β activates NF-κB signaling pathway leading to expression of several genes contributing to inflammation, immune response, and cell proliferation. Modulation of IKK-β kinase activity could be useful for treatment and management of such diseases. Starting from a discovered weakly active hit compound, twenty four thiazolidinedione-scaffold based chemical entities belonging to five series have been designed, synthesized and evaluated as potential IKK-β modulators. Among them, compounds **6q**, **6r** and **6u** showed low micromolar IC_{50} values while compounds **6v**, **6w**, and **6x** elicited submicromolar IC_{50} values equal to 0.4, 0.7 and 0.9 µM respectively. These submicromolar IC_{50} values are 243, 139 and 105 folds the value of the reported IC_{50} of the starting hit compound. Kinetic study of compounds **6v** and **6w** confirmed this class of modulators as irreversible inhibitors. LPS-treated RAW 264.7 macrophages proved the anti-inflammatory activity of compounds **6q** and **6v.** Assay of hERG inhibition demonstrated a safe profile of compound **6q** suggesting it as a lead for further development of IKK-β modulators.

Keywords

IKK-β modulators, NF-κB signaling pathway, Thiazolidinediones, Allosteric modulation

1. Introduction

Protein kinases constitute the third largest class of enzymes as more than five hundred kinases have been identified in human kinome [1]. They are estimated to phosphorylate not less than 30% of the human proteome [2]. Anomalous phosphorylations are linked with numerous diseases such as cancer, neurological disorders, diabetes, inflammation and rheumatoid arthritis. Consequently, modulation of protein kinases has been the target of several drug development programs. Currently, the majority of developed kinase inhibitors compete with ATP to its binding site. Because of ATP binding pockets similarities across kinases, it is a challenging task to develop the specific inhibitor of a single kinase. This could limit the clinical applicability of the developed molecules [3]. In contrast, modulation of kinases *via* allosteric sites has recently evolved as an alternative strategy that offers the possibility for overcoming the selectivity issue encountered with the classical modulators binding to the ATP pocket [4, 5].

IKK-β (Inhibitor of nuclear factor kappa-B kinase subunit beta) is a kinase that activates the transcription factor NF-κB (nuclear factor kappa-light-chain-enhancer of activated B cells) through phosphorylation of IκB (inhibitor of NF-κB). As a consequence, degradation of the IκB subunit is triggered releasing NF-κB [6]. The free NF-κB translocates to the nucleus and induces expression of over five hundred genes including genes encoding for several inflammatory response mediators such as chemokines (CCL5, CCL20, CXCL8 and CXCL10), cytokines (TNF-α, IL-1β and IL-6), and adhesion molecules (VCAM, ICAM and ELAM), in addition to the enzymes inducible nitric oxide synthase (iNOS) and cyclooxygenase-2 (COX2) [7, 8]. Consequently, NF-κB pathway modulators have been suggested as an approach for treatment of acute, as well as, chronic inflammatory diseases [9, 10]. In addition to its contribution to the development of inflammatory conditions, NF-κB-

induced genes expression is also involved in immune response, cells' proliferation, oncogenesis, apoptosis and viral infections [11]. Therefore, modulation of NF-κB is a useful tool for addressing multiple pathological conditions. Modulation of NF-κB might be achieved through several strategies including modulation of kinases and phosphatases involved in NF-κB signaling pathway, as well as, targeting the processes of ubiquitination, nuclear translocation, DNA binding, acetyl and methyl transferases which are required for NF-κB triggered genes expression [7, 8].

Modulation of the kinase IKK-β has received attention as it is a limiting point in NF-κB signaling pathway and thus is a potential therapeutic target [12, 13]. In fact, IKK-β acts not only on IκB proteins, but acts also on other several substrates including SNAP23, TSC1, Foxo3a, TLP2, IRS-1 [14, 15]. Accordingly, it participates in NF-κB-independent signals to modulate mast cell degranulation, inflammation mediated angiogenesis, cell cycle arrest, MAPK, and insulin resistance respectively. Previous drug discovery programs initiated by several research groups afforded IKK-β inhibitors belonging to various chemical scaffolds [13]. However, to the best of our knowledge, almost all of these developed IKK-β inhibitors are orthosteric inhibitors such as phenylpyridinamine derivative (**1**) developed by Bayer (Fig. 1) [16]. The IKK-β allosteric modulators are scarce despite their apparent advantages over the orthosteric modulators. The imidazoquinoxaline derivative BMS-345541 (**2**) is a non-selective allosteric inhibitor of both IKK-α and IKK-β [8]. Recently, the complex natural product (+)-ainsliadimer (**3**) was found to allosterically inhibit IKK-β *via* conjugation to cysteine 46 (Cys46) present in the vicinity of the catalytic ATP binding pocket [17]. A drug discovery study by Park *et al.* reported 6-phenyl-1,3,5-triazine-2,4-diamine derivative (**4**) and 5-(2-indolyldiene)-2-imino-4-thiazolidinone derivative (**5**) as hit compounds inhibiting IKK-β with measured IC_{50} values equal to 7.8 and 97.4 μM respectively [18]. In their report, they

have considered development of only the more potent hit compound **4** into potential IKK-β inhibitors. The current study focuses on the development of the weakly active hit compound **5** as a starting point to afford novel thiazolidinedione derivatives as potential IKK-β modulators.

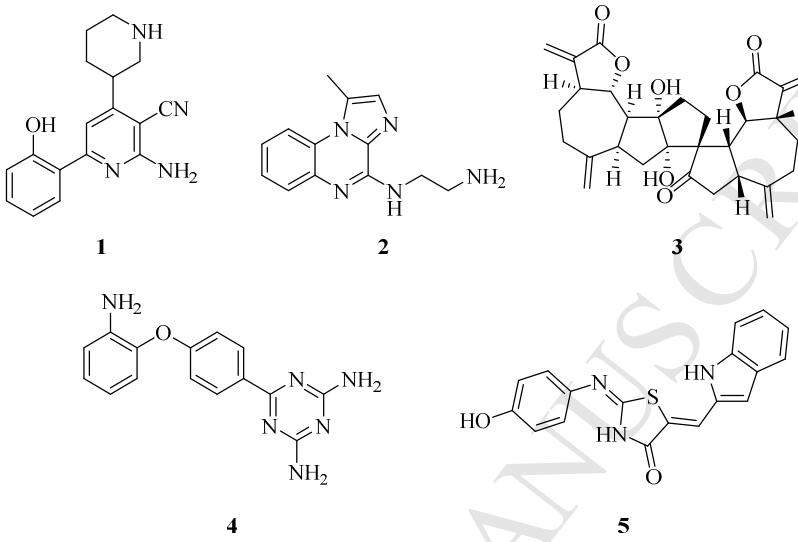

Fig. 1. Reported inhibitors and discovered hit compounds for IKK-β

2. Results and discussion

2.1. Ligands Design

The structure of the reported natural product allosteric inhibitor (+)-ainsliadimer (**3**) incorporates Michael acceptor moiety that covalently binds with Cys46 residue of IKK-β [17]. *In silico* study showed that covalent binding to Cys46 residues induces structural changes in the kinase domain of IKK-β. As the weakly active hit compound **5** possesses a Michael acceptor moiety, it may offers possibility to develop covalent allosteric modulators that could conjugate with Cys59 of IKK-β upon specific binding to this site.

To develop more potent ligands based on the structure of the hit compound **5**, rational modifications were planned as shown in Fig. 2. The indole moiety attached to the unsaturated

center might be replaced with phenyl ring. The effect of the introduced phenyl ring on the reactivity of the Michael acceptor moiety towards conjugation with Cys46 to inhibit IKK-β might be modulated by the phenyl ring substituents. Different substituted-phenoxy moieties, as well as, morpholino and halo substituents were planned. Displacement of the 4-hydroxyphenyl moiety present in the starting hit compound from position 2 to position 3 might affect the reactivity of the Michael acceptor center through reduction of the electron density on the nitrogen atom of the α,β-unsaturated amide moiety. Also, elimination of the imine functionality might provide more stable compounds, yet maintain the desirable bioactivity. Linking various piperazine derivatives to the 4-hydroxyphenyl moiety would permit better balance of hydrophobic-hydrophilic characters of the designed ligands.

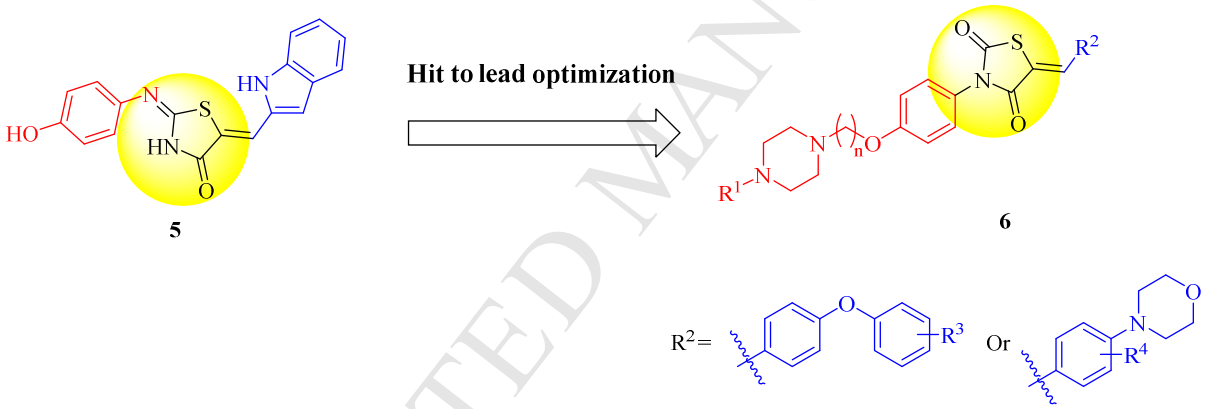

Fig. 2. Design of the novel thiazolidinedione derivatives

2.2. Chemistry

Synthesis of the designed derivatives (**6**) was achieved by a sequence of six steps as shown in Scheme 1. First, reaction of commercially available 4-aminophenol (**7**) with chloroacetyl chloride at 0 °C afforded 2-chloro-*N*-(4-hydroxyphenyl)acetamide (**8**). Tandem reaction with potassium salt of thiocyanate yielded the cyclized 3-(-4-hydroxyphenyl)-2-iminothiazolidin-4-one (**9**) *via* nucleophilic substitution of the chlorine atom with the thiocyanate radical followed by nucleophilic addition of the amide's nitrogen to the electrophilic carbon of the

thiocyanate moiety [19]. Acid catalyzed hydrolysis of the 2- imino moiety provided the targeted core; 3-(4-hydroxyphenyl)thiazolidine-2,4-dione (**10**) [20]. Introduction of the desired piperazinyl moieties required first installation of a linker *via O*-alkylation of the phenolic hydroxyl group in a refluxing acetonitrile solution with 1,n-diiodoalkanes in presence of potassium carbonate to afford the 4-(*N*-iodoalkoxy)phenyl derivatives (**11**) which were used to *N*-alkylate the appropriate 1-(substituted)piperazine derivatives in acetonitrile solution at room temperature employing potassium carbonate as a base to provide the corresponding 3-(4-(*N*-(4-substitutedpiperazin-1-yl)alkoxy)phenyl)thiazolidine-2,4-dione derivatives (**12**). Finally, sodium acetate catalyzed Knoevenagel condensation with the appropriate commercially available benzaldehyde derivative in acetic acid solution provided the targeted final compounds (**6**) [21].

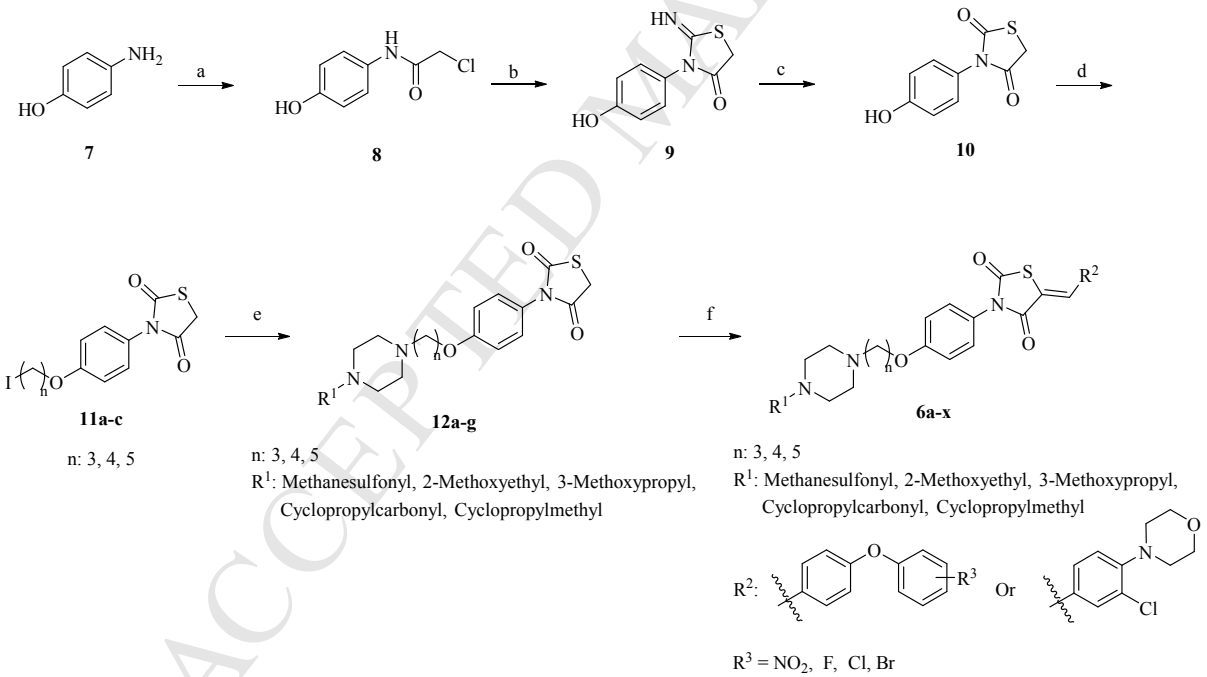

Scheme 1. Reagents and reaction conditions: (a) Chloroacetyl chloride, DCM, 0 °C, 1.5 h, rt, 3 h; (b) KSCN, acetone, 65 °C, 7 h; (c) 2% HCl aqueous solution, 100 °C, 7 h; (d) Diiodoalkane, K_2CO_3, MeCN, 95 °C, 7 h; (e) Appropriate piperazine derivative, K_2CO_3, MeCN, rt, 9 h; (f) Appropriate aldehyde derivative, NaOAc, AcOH, 110 °C, 16 h.

2.3. Biological evaluation

2.3.1. *In vitro* IKK-β induced phosphorylation modulation

The prepared final compounds belong to five different series on the basis of the piperazinyl moieties linked to the 4-hydroxyphenyl ring present at position 3 of the thiazolidine core *via* a four carbon atoms linker. Also, shorter and longer linkers (3 and 5 carbon atoms respectively) were used to prepare further derivatives of the series that elicited the highest activity. Thus, a total of twenty four final compounds were prepared and evaluated for their capability of *in vitro* modulation of the phosphorylation triggered by IKK-β. In this assay, the IκBα-derived substrate (5-FAMGRHDSGLDSMK-NH_2; R7574, MDS Analytical Technologies) which is labeled with 5-FAM (5-carboxyfluorescein) was used as a substrate for IKK-β employing an IMAP® based fluorescent assay that is based on the specific high-affinity of a trivalent metal immobilized on nanoparticles to bind the phosphorylated substrate [22]. To ensure the sensitivity of the performed assay, it was conducted as a TR-FRET assay (time-resolved Förster resonance energy transfer assay) [23]. Because percent inhibition and IC_{50} values of irreversible inhibitors increase over time, measurements were acquired after two hours to allow completion of reaction. The outcome results of the assay is displayed in Table 1 and illustrated in Fig. 3.

Table 1. Results of IKK-β TR-FRET and hERG assays

Cpd	n	R^1	R^2	IKK-β assay		hERG assay		Safety Index[c]
				% Inhibition[a]	IC_{50} (μM)	% Inhibition[b]	IC_{50} (μM)	
6a	4		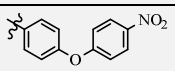	0.0	—	—	—	—
6b	4		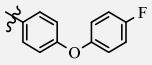	2.7	—	—	—	—
6c	4		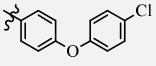	0.8	—	—	—	—
6d	4		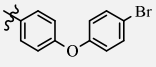	3.3	—	—	—	—
6e	4		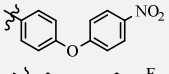	9.3	—	—	—	—
6f	4		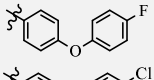	1.6	—	—	—	—
6g	4		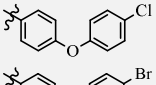	1.7	—	—	—	—
6h	4		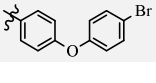	0.0	—	—	—	—

6i	4	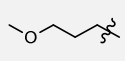	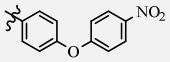	9.4	—	—	—	—
6j	4	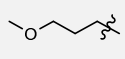	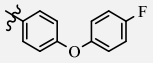	0.7	—	—	—	—
6k	4	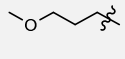	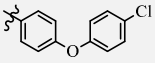	1.6	—	—	—	—
6l	4	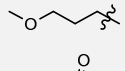	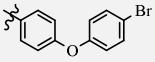	0.0	—	—	—	—
6m	4		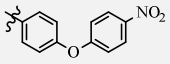	21.7	—	—	—	—
6n	4		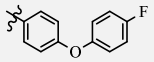	21.2	—	—	—	—
6o	4		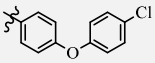	17.0	—	—	—	—
6p	4		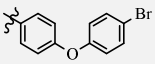	52.4	8.6	17.1	—	—
6q	4		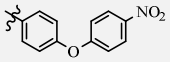	85.6	1.5	61.2	55.3	36.9
6r	4		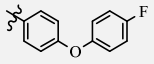	85.7	1.7	99.5	3.4	2.0
6s	4		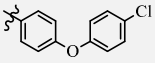	37.5	—	—	—	—
6t	4		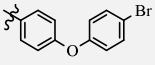	60.8	7.9	66.5	27.5	3.5
6u	3		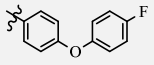	88.8	1.4	—	—	—
6v	5		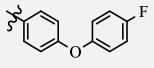	92.8	0.4	—	—	—
6w	3		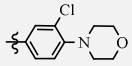	90.7	0.7	—	—	—
6x	5		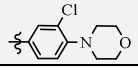	92.1	0.9	—	—	—

[a] % Inhibition of 10 μM concentrations
[b] % Inhibition of 100 μM concentrations
[c] Calculated safety index for hERG inhibition by dividing values of IC_{50} of hERG inhibition by IC_{50} of IKK-β inhibition.

As shown in Fig. 3, the elicited bioactivities of 10 μM concentrations of the tested compounds, although not fully understood, showed large variations depending on the type of the *N*-substituents of piperazine moiety. Compounds having piperazinyl moiety bearing 4-methanesulfonyl substituent were almost inactive. Although that ligands belonging to the 4-(2-methoxyethyl)piperazin-1-yl and 4-(3-methoxypropyl)piperazin-1-yl series (both are less polar piperazinyl moieties relative to the 4-(methanesulfonyl)piperazin-1-yl moiety) were also inactive compounds, derivatives **6e** and **6i** bearing 4-nitrophenyloxy substituent on the ring of the 5-benzylidene moiety showed weak activity at the tested 10 μM concentration. It

is known that nitro group is more electron withdrawing group than the electronically amphiphilic halo-groups present in other members of this series. Decreasing the polarity of the 4-(substituted)piperazin-1-yl moiety by switching its 4-substituent to cyclopropylcarbonyl resulted in a noticeable enhancement of the measured phosphorylation inhibition of the substrate by IKK-β by all of the prepared derivatives of this series (**6m**−**p**) relative to corresponding derivatives **6a**−**d, 6e**−**6h**, and **6i**−**l**. The value of the elicited inhibition by nitro derivative **6m** was more than double the value elicited by nitro derivatives **6e** and **6i**. Also, the activity of the halogenated derivatives **6n**−**6p** became significant while the corresponding derivatives of the methansufonyl, 2-methoxyethyl and 3-methoxyethyl series were almost negligible. The most active derivative among the prepared derivatives of the cyclopropylcarbonyl series was the bromo derivative **6p** which elicited IC_{50} value equals to 8.58 µM. Relative to the initial hit compound which had IC_{50} equals to 97.4 µM, this represented a milestone towards enhancement of the IKK-β inhibitory activity. Further decrease of the polarity of 4-(substituted)piperazin-1-yl moiety by replacing the cyclopropylcarbonyl group with cyclopropylmethyl resulted in a great enhancement of the measured percent inhibition. Almost all of the prepared derivatives belonging to the cyclopropylmethyl series showed high percent inhibition and low micromolar or submicromolar IC_{50} values. The nitro derivative **6q** and the fluoro derivative **6r** elicited approximately similar high percent inhibition and low micromolar IC_{50} values. The other prepared halogenated derivatives exhibited lower inhibition percent but higher IC_{50} values relative to the fluoro derivative **6r**. Shortening or extending the linker of the fluoro derivative **6r** by one carbon afforded another two highly active analogues **6u** and **6v** respectively. While analogue **6u** having the shorter linker showed a high percent inhibition and a low micromolar IC_{50} value which was close to that of compound **6r**, the extended linker analogue **6v** was the most potent compound among the prepared compounds exhibiting the highest percent

inhibition and a submicromolar IC_{50} value. As we observed that the active compounds **6q** and **6r** had highly electronegative fluoro or nitro substituents, we explored the effect of switching from 4-(phenyl)oxy substituents to other groups with different electronic properties. Accordingly, derivatives **6w** and **6x** in which 3-chloro and 4-morpholinophenyl substituents replaces the 4-(phenyl)oxyphenyl substituents present in derivatives **6a**−**v** were prepared and evaluated. Both **6w** and **6x** elicited high inhibition percent and submicromolar IC_{50} values of 0.7 and 0.9 µM respectively indicating electron withdrawing group at position 3 would result in active compounds despite the presence of electron donating group at position 4.

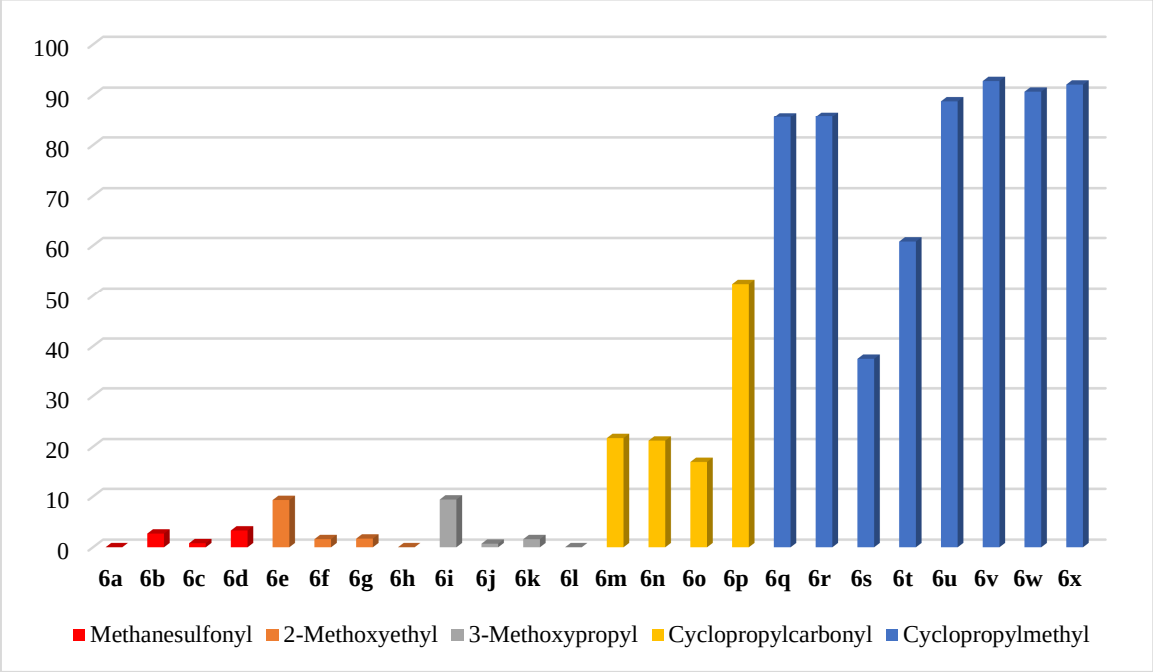

Fig. 3. % Inhibition of IKK-β measured at 10 µM concentrations of the synthesized compounds

2.3.2. Kinetic study of IKK-β inhibition

To confirm the irreversible nature of IKK-β inhibition induced by the synthesized compounds, a kinetic study was conducted using the potent inhibitors **6v** and **6w**. Thus, the percent inhibition produced by ten doses (30, 10, 3, 1, 0.3, 0.1, 0.03, 0.01, 0.003 and 0.001 µM concentrations) was measured at 0, 20, 40 and 60 min intervals. As Fig. 4 illustrates, the dose

response curves showed an increase in percent inhibition upon increasing the reaction time which elucidates that these compounds are IKK-β irreversible inhibitors. The parameters of the time-dependent dose response curves are displayed in Table 2. All curves obtained from the acquired data possessed high correlation values (R^2 = 0.9793~0.9961) with 95% confidence spanning almost all of the measured ranges. According to the calculated parameters, the rate of conjugation reaction of compound **6w** to cysteine residue is higher than the rate of compound **6v** reaction as the slopes of the dose response curves of the **6w** is higher than those for compound **6v** at any corresponding time. This may be reflect the effect of the substituents on the benzylidene moiety as compound **6v** has 4-fluorophenoxy substituent while compound **6w** has 3-chloro-4-morpholino substituent. As a result, at zero minute time, compound **6v** has pIC_{50} ($-LogIC_{50}$) lower than that of compound **6w**. However, as time increases, the pIC_{50} value of compound **6v** increases to until it slightly surpass approximates that of compound **6w** at 60 min. time (pIC_{50} = 6.619 and 6.598 for **6v** and **6w** respectively). Next, we used data of time dependent response curves to calculate the values for K_{obs} for each concentration of compounds **6v** and **6w** according to the equation where: ln(%enzyme activity remained) = $-K_{obs} \times$ time + α. Plotting these calculated K_{obs} values and performing a nonlinear regression against concentration as shown in Fig. 4C and 4D provided the K_{inact} values according to the equation: $K_{obs} = K_{inact} \times [\ I\ ] / (K_i + [\ I\ ])$ [24]. The K_{inact} values were 0.039 and 0.021 (min^{-1}) for compounds **6v** and **6w** respectively.

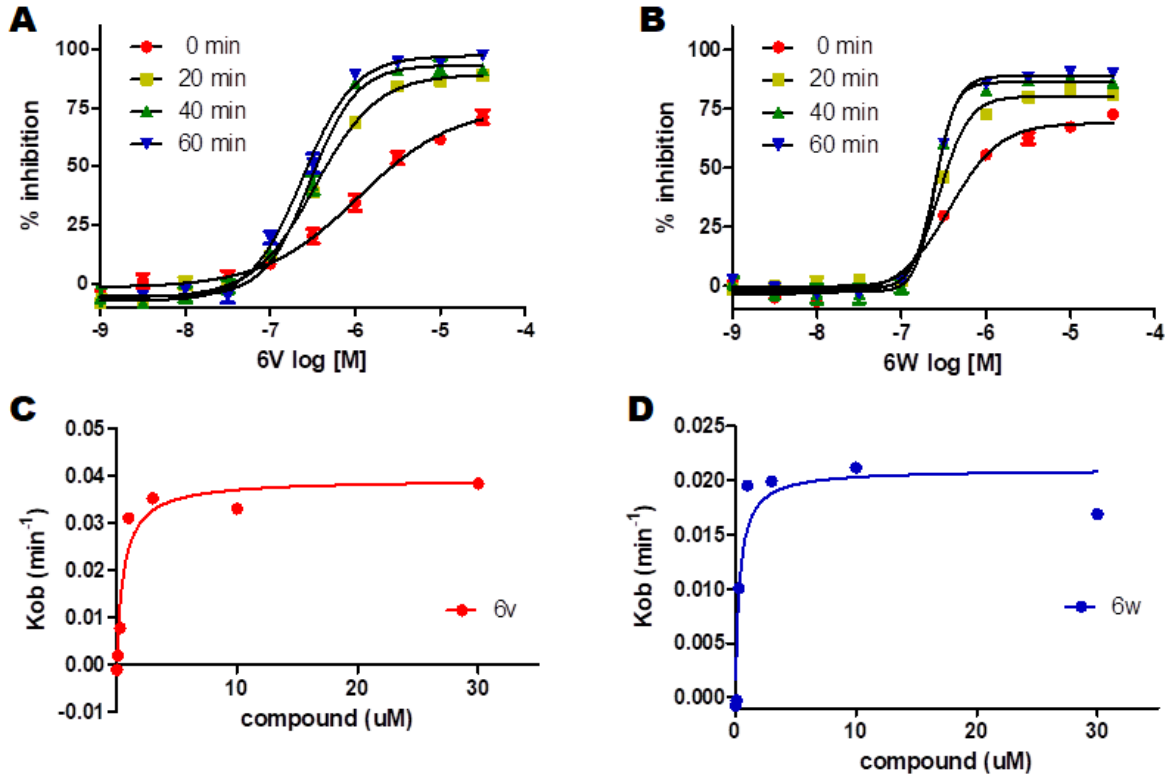

Fig. 4. A) Time-dependent dose-responses curves of compound **6v**. B) Time-dependent dose-responses curves of compound **6w**. C) Nonlinear regression of calculated K_{obs} values against concentration of compound **6v**. D) Nonlinear regression of calculated K_{obs} values against concentration of compound **6w**.

Table 2. Parameters of the time-dependent dose response curves for inhibition of IKK-β by compounds **6v** and **6w** measured by TR-FRET assay

Compound		**6v**				**6w**			
Time intervals		0 min	20 min	40 min	60 min	0 min	20 min	40 min	60 min
Best-fit values	Bottom	-1.639	-5.837	-5.296	-7.21	-3.349	-0.08157	-2.344	-1.254
	Top	75.66	89.4	93.29	97.41	69.05	80.35	86.38	89.09
	-LogIC$_{50}$	5.96	6.468	6.525	6.619	6.429	6.541	6.601	6.598
	HillSlope	0.7724	1.191	1.599	1.418	1.473	2.505	3.744	3.302
	Span	77.3	95.24	98.58	104.6	72.4	80.43	88.72	90.34
Std. Error	Bottom	1.66	1.222	1.559	1.468	1.181	0.9616	1.131	0.8308
	Top	4.305	1.542	1.806	1.605	1.489	1.05	1.143	0.8458
	Span	5.213	2.15	2.534	2.327	2.028	1.495	1.642	1.217
95% Confidence Intervals Span		66.58 ~ 88.01	90.82 ~ 99.66	93.37 ~ 103.8	99.83 ~ 109.4	68.23 ~ 76.57	77.36 ~ 83.50	85.34 ~ 92.10	87.84 ~ 92.84
Goodness of Fit	DF[a]	26	26	26	26	26	26	26	26
	R^2	0.9793	0.9932	0.9888	0.992	0.9875	0.9932	0.9926	0.9961

[a] DF: Degrees of Freedom

2.3.3. Cellular assays for anti-inflammatory activity

In order to investigate the capability of the synthesized IKK-β inhibitors to alleviate inflammation at the cellular level, LPS-induced inflammatory responses in RAW 264.7 macrophages was employed as a model. It is well established that treatment of RAW 264.7 macrophages with LPS stimulates NF-κB signaling pathway resulting in production of inflammatory mediators including TNF-α [25] and PGE_2 [26]. For performing cellular assays, three doses (1.5, 3 and 6 µM) of **6q**, **6v**, **6w** and **6x** were used for evaluation. The results are illustrated in the following sections.

2.3.3.1. Impact on RAW 264.7 macrophages Cells' Viability

For accurate determination of the candidate compounds ability to reduce the production of the inflammatory mediators, it is crucial to exclude the reduction caused by non-specific cytotoxicity. Accordingly, the impact of compounds on the cells' viability was investigated at the concentrations used for determination of PGE_2 and TNF-α production. As shown in Fig. 5, in presence of only compound **6q** or **6v**, there was no effect on cell viability at the highest concentration employed (6 µM). Also, for compounds **6q** and **6v**, there was no cytotoxic activity in presence of both of LPS and the candidate compound over the range of concentrations used in the subsequent experiments. Although compound **6w** did not produce any cytotoxicity at 6 µM concentration, cytotoxicity was observed upon using combining LPS with this concentration. Moreover, the cell viability testing revealed that compound **6x** elicits cytotoxic effect on RAW 264.7 macrophages in absence of LPS and this cytotoxicity increased upon presence of LPS. As Table 3 indicates, the concentrations of **6w** and **6x** that decrease cells viability to 80% in presence of 1 µg/ml of LPS (IC_{80}) were 2.67 and more than 1.5 µM, respectively.

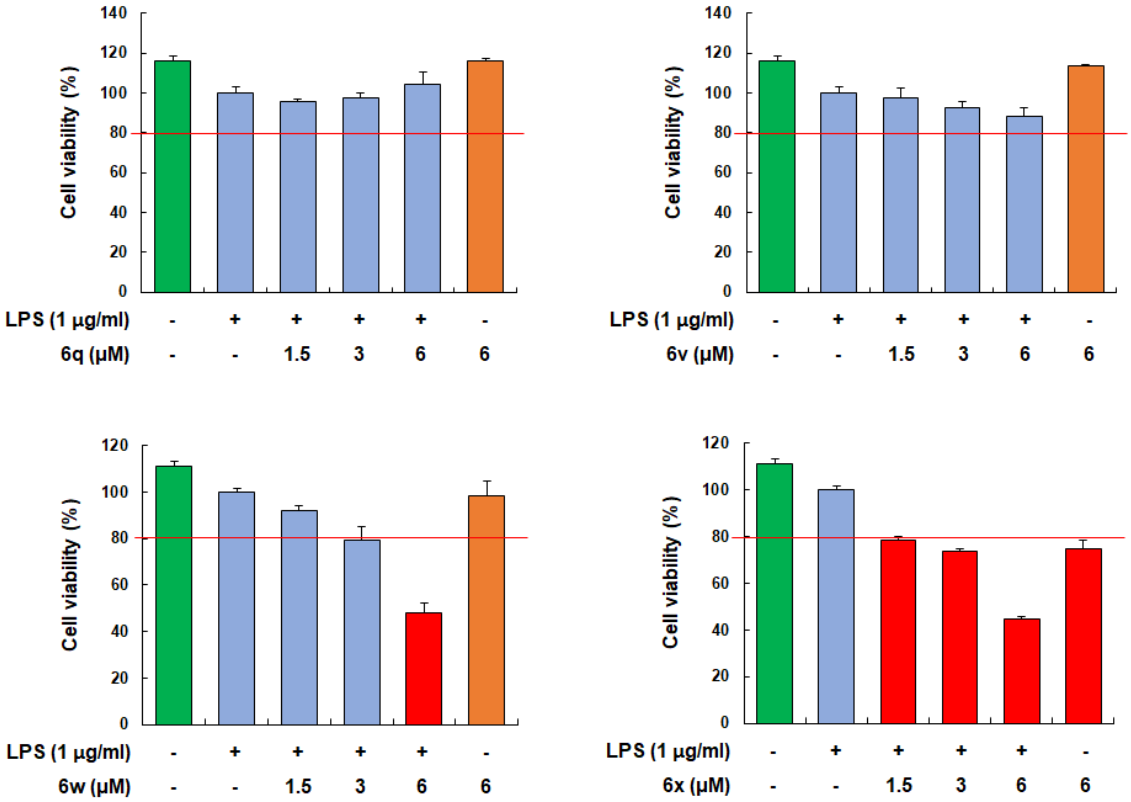

Fig. 5. Viability of RAW 264.7 macrophage cells: in presence of LPS (green color), in presence of 6 µM of tested compounds (dark buff color) and in presence of both of LPS and tested compounds (cyan color). Red color indicates cytotoxicity of macrophages cells (viability percent below 80%).

Table 3. Viability of RAW 264.7 macrophages and IC_{50} for reduction of production of PGE2 and TNF-α

Compound	IC_{80} [a] (µM)	IC_{50} [b] (µM)	
	Cell viability	PGE_2	TNF-α
6q	> 6	> 6	3.41
6v	> 6	> 6	1.67
6w	2.67	NC[c]	> 6
6x	< 1.5	> 6	NT[d]

[a] IC_{80}: defined as the concentration of the compound that decreases viability of cells to 80% in presence of 1 µg/ml of LPS.
[b] IC_{50}: defined as the concentration that decreases the measured amount of produced PGE_2 or TNF-α to 50%
[c] NC: Not calculated
[d] NT: Not tested

2.3.3.2. Effect on LPS-induced PGE_2 production in RAW 264.7 macrophages

Production of PGE_2 in microphages is a downstream of both mitogen-activated protein kinase (MAPK) and NF-κB signaling pathways [27]. Therefore, inactivation of NF-κB signaling pathway might result in reduction of PGE_2 production. To investigate the ability of the

synthesized compounds to reduce PGE_2 production, the amounts of PGE_2 produced in nanogram per mL were determined before and after stimulation of macrophages with LPS, as well as, in the presence of combination with LPS and variable doses of candidate compounds or standard NS-398 [28]. As shown in Fig. 6, production of PGE_2 was hardly detected in non-stimulated macrophages and also in presence of 6 µM concentrations of each of the four candidate compounds. As expected, upon LPS stimulation, PGE_2 production markedly increased. Upon using variable doses of candidate compounds, a significant dose-dependent reduction of PGE_2 was detected for all of the four candidate compounds. However, the reduction of PGE_2 production was less pronounced relative to that observed in case of the positive control inhibitor compound. As shown in Table 3, IC_{50} values were more than 6 µM. This low potency might arise from LPS-stimulation of other pathways contributing to production of PGE_2 other than NF-κB signaling pathways.

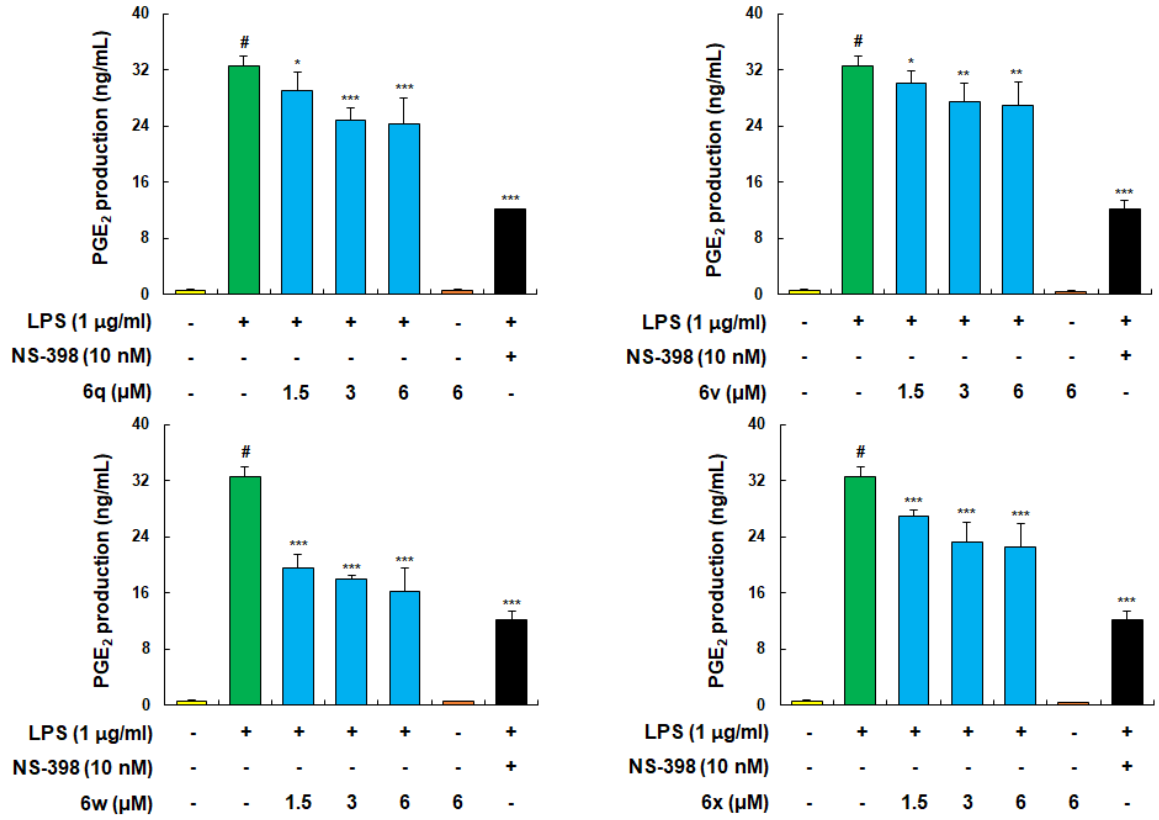

Fig. 6. Inhibitory effects of candidate compounds on lipopolysaccharide (LPS)-induced PGE_2 production in RAW 264.7 macrophages: yellow color indicates absence of LPS, candidate compounds or standard; dark buff color indicates presence of only candidate compound; green color indicates presence of only LPS; cyan color

indicates presence of a candidate compound and LPS; black color indicates presence of standard and LPS.

2.3.3.3. Effect on LPS-induced TNF-α production in RAW 264.7 macrophages

The cytokine TNF-α is a mediator of inflammation produced upon stimulation of several signaling pathways including NF-κB and Raf-1/MEK1-MEK2/ERK1-ERK2 [29, 30]. Abrogation of NF-κB activation through inhibition of IKK-β might assist in reduction of this proinflammatory cytokine and alleviate inflammation. Evaluation results of compounds **6q**, **6v** and **6w** to reduce TNF-α production are shown in Fig. 7. When LPS was added to macrophage cells, the detectable amount of TNF-α increased to 1.3 ng/mL. Significant dose dependent reduction of the produced TNF-α was elicited by compounds **6q** and **6v**. Although the reduction of TNF-α production was less prominent in case of compound **6w**, it was also significant. As shown in Table 3, compounds **6q** and **6v** produced IC_{50} values were 3.41 and 1.67 μM respectively. Collectively, the cellular assay results confirm that **6q** and **6v** possess significant cellular anti-inflammatory activity resulting in reduction of PGE_2 and TNF-α production without non-specific toxicity. Our cell based finding demonstrates that **6w** as a non-cytotoxic IKK-β inhibitor elicits higher reduction of PGE_2 production than compounds **6q** and **6v**, but with less ability to reduce TNF-α production than them.

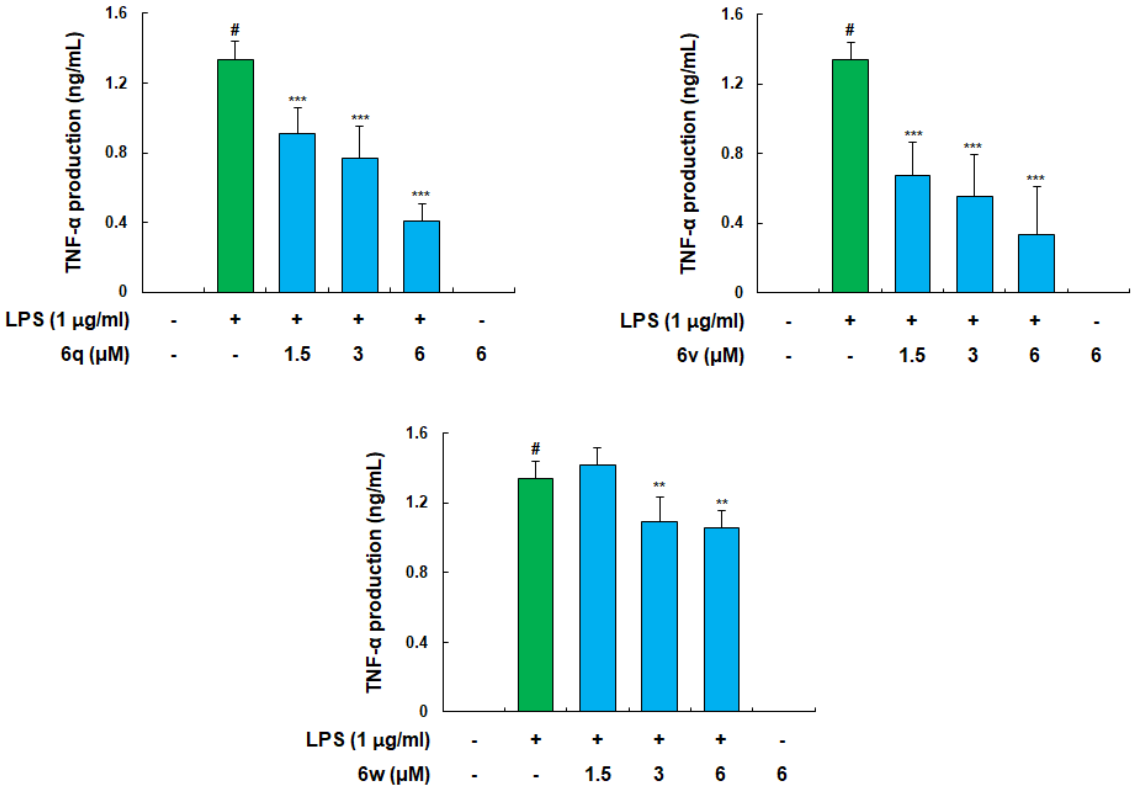

Fig. 7. Inhibitory effects of candidate compounds on lipopolysaccharide (LPS)-induced TNF-α production in RAW 264.7 macrophages: green color indicates presence of only LPS; cyan color indicates presence of a candidate compound and LPS.

2.3.4. Assessment of cardiosafety (hERG inhibition assay)

The cardiac potassium ion channel; known as hERG after the human ether-a-go-go-related gene which encodes this channel, has distinct kinetics that is crucial for repolarization of cardiac muscles. Unfortunately, hERG channel can be blocked by several drugs despite the absence of a clear structural and functional correlation [31-33]. This inhibition induces prolongation of QT interval that leads to the fatal torsades de pointes cardiac arrhythmia [33]. In fact, inhibition of hERG potassium channel is one of the major reasons for drug failure and withdrawal [34]. Apparently, early evaluation of hERG inhibition is required to minimize the failure rate of candidates that may arise in later stages of drug development. Because of the pivotal significance of hERG inhibition in clinical safety, we have evaluated the percent inhibition exhibited by a set of active compounds at an elevated concentration as high as of

100 µM and determined their IC_{50} values on hERG channel. As shown in Table 1, the concentration of nitro derivative **6q** required to produce 50% inhibition of hERG channel was 36.9 folds higher than the concentration required to inhibit 50% of kinase activity of IKK-β. This indicates an excellent safety index for nitro derivative **6q**. It should be mentioned that the bromo derivative **6p** was very safe regarding hERG inhibition as the inhibition percent at the high 100 µM concentration did not exceed 17.1%. Therefore, no IC_{50} was calculated for this derivative. However, with IC_{50} for inhibition of IKK-β equals to 8.6 µM, this compound might be not sufficiently potent for further development as IKK-β modulator. Unfortunately, the ratio of IC_{50} of hERG inhibition to the IC_{50} of IKK-β inhibition elicited by the fluoro derivative **6r** and the bromo derivative **6t** showed low safety index of 2.0 and 3.5 respectively. Based on these results, derivative **6q** might be a safe and potential candidate lead compound for development of modulators of IKK-β kinase reaction.

3. Conclusion

Using the hit compound **5** as a starting point, potential allosteric covalent IKK-β modulators were developed. Relative to the starting hit compound, derivatives **6q**, **6r** and **6u** elicited enhanced activity by 57~69 folds showing low micromolar IC_{50} values within the range of 1.4~1.7 µM . In addition, derivatives **6w**, and **6x** showed submicromolar IC_{50} values within the range of 0.7~0.9 µM, which is 139 and 105 folds enhanced values. The most potent compound **6v** exhibited enhanced activity by more than 243 folds eliciting submicromolar IC_{50} values of 0.4 µM. Kinetic study of the inhibition produced by compounds **6v** and **6w** over 20 minutes intervals confirmed their irreversible mode of action. Cellular assays presented compounds **6q** and **6v** as anti-inflammatory agents suppress both LPS-induced PGE_2 and TNF-α production without non-specific cytotoxicity. For development of ligands devoid of cardiotoxicity, assay for inhibition of hERG was performed which present the safe

and active anti-inflammatory compound **6q** as a lead for further development of anti-inflammatory modulators of IKK-β.

4. Experimental

4.1. Chemistry

General: All reactions and manipulations were performed using standard Schlenk techniques. Solvents and reagents were purchased from commercial suppliers and used without further purification. The NMR spectra were obtained on Bruker Avance 400. ^{1}H NMR spectra were referenced to tetramethylsilane (δ = 0.00 ppm) as an internal standard and are reported as follows: chemical shift, multiplicity (br = broad, s = singlet, d = doublet, t = triplet, dd = doublet of doublet, m = multiplet). Column chromatography was performed on Merck Silica Gel 60 (230−400 mesh) and eluting solvents for all of these chromatographic methods are noted as appropriated-mixed solvent with given volume-to-volume ratios. TLC was carried out using glass sheets pre-coated with silica gel 60 F_{254} purchased by Merk.

2-Chloro-*N*-(4-hydroxyphenyl)acetamide (8). Chloroacetyl chloride (13 mL, 0.17 mol) was slowly added to a suspension of 4-aminophenol (**7**, 15 g, 0.14 mol) in anhydrous dichloromethane (50 mL) at 0 ^{o}C. The reaction mixture was stirred at 0 ^{o}C for 1.5 h and at room temperature for 3 h. The reaction mixture was added to saturated sodium hydrogen carbonate aqueous solution and then extracted with ethyl acetate. The organic layer was evaporated under reduced pressure. The residue was washed with water and dried to yield the desired product (white solid, 64%, 16.3 g). ^{1}H NMR (400 MHz, DMSO-d_6) δ: 4.19 (s, 2H), 6.72 (d, J = 8.8 Hz, 2H), 7.37 (d, J = 8.8 Hz, 2H), 9.30 (s, 1H), 10.04 (s, 1H). ^{13}C NMR (100.6 MHz, DMSO-d_6) δ: 43.5, 115.2, 121.2, 130.0, 153.8, 163.9. HRMS (ES+): *m/z* calculated for $C_8H_8ClNO_2$: 208.0142 $[M+Na]^+$. Found 208.0134.

3-(-4-Hydroxyphenyl)-2-iminothiazolidin-4-one (9). Potassium thiocyanate (7.8 g, 80.8 mmol) was added to a solution of 2-chloro-*N*-(4-hydroxy-phenyl)acetamide (**8**, 10 g, 53.9 mmol) in acetone (30 mL) and the reaction mixture was refluxed for 7 h. The solvent was evaporated under reduced pressure and the residue was suspended in water, filtered, and dried to give the title compound (white solid, 68%, 7.6 g). ^{1}H NMR (400 MHz, DMSO-d_6) δ: 4.11 (s, 2H), 6.83 (d, J = 8.6 Hz, 2H), 7.02 (d, J = 8.6 Hz, 2H), 9.14 (s, 1H), 9.68 (s, 1H). ^{13}C NMR (100.6 MHz, DMSO-d_6) δ: 33.9, 115.9, 126.7, 130.0, 157.6, 158.9, 172.2. HRMS (ES+): *m/z* calculated for $C_9H_8N_2O_2S$: 209.0384 $[M+H]^+$. Found 209.0381.

3-(4-Hydroxyphenyl)thiazolidine-2,4-dione (10). 3-(4-Hydroxyphenyl)-2-iminothiazolidin-4-one (**9**, 3.6 g, 17.3 mmol) was dissolved in 2% hydrochloride aqueous solution (37 mL) and the mixture was stirred at 100 ^{o}C for 7 h. After cooling, the reaction mixture was neutralized to pH 7 using aqueous solution of sodium bicarbonate, filtered and dried to give the title compound (white solid, 55%, 2 g). ^{1}H NMR (400 MHz, DMSO-d_6) δ: 4.26 (s, 2H), 6.83 (d, J = 8.8 Hz, 2H), 7.06 (d, J = 8.8 Hz, 2H), 9.79 (s, 1H). ^{13}C NMR (100.6 MHz, DMSO-d_6) δ: 34.0, 115.6, 124.3, 129.0, 157.8, 171.6, 172.1.

General procedure of 3-(4-(*N*-iodoalkoxy)phenyl)thiazolidine-2,4-dione (11). Potassium carbonate (3.7 g, 26.8 mmol) was added to a solution of 3-(4-hydroxyphenyl)-thiazolidine-2,4-dione (**10**, 2.8 g, 13.4 mmol) in acetonitrile (20 mL) and stirred for 10 min. Diiodoalkane (80.3 mmol) was added and the reaction mixture was stirred at 95 ^{o}C for 7 h. After cooling, water (10 mL) was added followed by extraction with ethyl acetate. The organic layer was dried over anhydrous $MgSO_4$, filtered and evaporated under reduced pressure. The residue was purified by flash column chromatography (SiO_2, *n*-hexane/ethyl acetate 3:1 v/v) to afford

the desired compounds.

3-(4-(3-Iodopropoxy)phenyl)thiazolidine-2,4-dione (11a). White solid, yield: 81%, 4.0 g, ^{1}H NMR (400 MHz, DMSO-d_6) δ: 2.19−2.24 (m, 2H), 3.39 (t, *J* = 6.6 Hz, 2H), 4.06 (t, *J* = 4.7 Hz, 2H), 4.28 (s, 2H), 7.05 (d, *J* = 7.1 Hz, 2H), 7.20 (d, *J* = 7.1 Hz, 2H). HRMS (ES+): *m/z* calculated for $C_{12}H_{12}INO_3S$: 399.9481 $[M+Na]^+$. Found 399.9472.

3-(4-(4-Iodobutoxy)phenyl)thiazolidine-2,4-dione (11b). White solid, yield: 72%, 3.7 g, ^{1}H NMR (400 MHz, $CDCl_3$) δ: 1.82 (br, 2H), 1.93 (br, 2H), 3.18 (br, 2H), 3.92 (br, 2H), 3.99 (s, 2H), 6.89 (d, *J* = 7.0 Hz, 2H), 7.06 (d, *J* = 7.0 Hz, 2H). ^{13}C NMR (100.6 MHz, $CDCl_3$) δ: 6.4, 30.1, 33.8, 67.0, 115.3, 125.3, 128.5, 159.4, 170.9, 171.3. HRMS (ES+): *m/z* calculated for $C_{13}H_{14}INO_3S$: 413.9691 $[M+Na]^+$. Found 413.9641.

3-(4-(5-Iodopentyloxy)phenyl)thiazolidine-2,4-dione (11c). White solid, yield: 88%, 4.6 g, ^{1}H NMR (400 MHz, $CDCl_3$) δ: 1.51–1.54 (m, 2H), 1.74–1.75 (m, 4H), 3.14 (t, *J* = 7.0 Hz, 2H), 3.91 (t, *J* = 6.0 Hz, 2H), 4.02 (s, 2H), 6.90 (d, *J* = 8.0 Hz, 2H), 7.08 (d, *J* = 8.0 Hz, 2H). ^{13}C NMR (100.6 MHz, $CDCl_3$) δ: 6.6, 27.1, 28.1, 33.1, 33.8, 67.9, 115.3, 125.1, 128.4, 159.5, 170.9, 171.3. HRMS (ES+): *m/z* calculated for $C_{14}H_{16}INO_3S$: 427.9794 $[M+Na]^+$. Found 427.9792.

General procedure of 3-(4-(*N*-(4-substitutedpiperazin-1-yl)alkoxy)phenyl)thiazolidine-2,4-dione (12). An appropriate piperazine derivative (1.34 mmol) and potassium carbonate (180 mg, 1.34 mmol) were added to a solution of the appropriate 3-(4-(*N*-iodoalkoxy)phenyl)thiazolidine-2,4-dione (**11**, 0.67 mmol) in acetonitrile (6 mL). The reaction mixture was stirred at room temperature for 9 h. The mixture was quenched by

addition of water and extracted with dichloromethane. The organic layer was dried over anhydrous $MgSO_4$, filtered and evaporated under reduced pressure. The residue was purified by column chromatography (SiO_2, DCM/MeOH 15:1 v/v including 1% of ammonium hydroxide).

3-(4-(4-(4-(Methylsulfonyl)piperazin-1-yl)butoxy)phenyl)thiazolidine-2,4-dione (12a). Yield: 77%, ^{1}H NMR (400 MHz, $CDCl_3$) δ: 1.56−1.60 (m, 2H), 1.73−1.76 (m, 2H), 2.36–2.39 (m, 2H), 2.40 (br, 4H), 2.85 (s, 3H), 2.08 (br, 4H), 4.02 (t, *J* = 6.4 Hz, 2H), 4.27 (s, 2H), 7.03 (d, *J* = 8.9 Hz, 2H), 7.19 (d, *J* = 8.9 Hz, 2H). HRMS (ES+): *m/z* calculated for $C_{18}H_{25}N_3O_5S_2$: 428.1314 $[M+H]^+$. Found 428.1322.

3-(4-(4-(4-(2-Methoxyethyl)piperazin-1-yl)butoxy)phenyl)thiazolidine-2,4-dione (12b). Yield: 42%, ^{1}H NMR (400 MHz, $CDCl_3$) δ: 1.62–1.69 (m, 2H), 1.77−1.82 (m, 2H), 2.40 (t, *J* = 7.3 Hz, 2H), 2.45–2.60 (m, 10H), 3.35 (s, 3H), 3.50–3.52 (m, 2H), 3.93 (t, *J* = 6.3 Hz, 2H), 4.10 (s, 2H), 6.97 (d, *J* = 8.8 Hz, 2H), 7.14 (d, *J* = 8.8 Hz, 2H). HRMS (ES+): *m/z* calculated for $C_{20}H_{29}N_3O_4S$: 408.1957 $[M+H]^+$. Found 408.1955.

3-(4-(4-(4-(3-Methoxypropyl)piperazin-1-yl)butoxy)phenyl)thiazolidine-2,4-dione (12c). Yield: 55%, ^{1}H NMR (400 MHz, $CDCl_3$) δ: 1.62–1.70 (m, 2H), 1.73–1.82 (m, 4H), 2.40–2.60 (m, 12H), 3.32 (s, 3H), 3.41 (t, *J* = 6.4 Hz, 2H), 3.99 (t, *J* = 6.4 Hz, 2H), 4.10 (s, 2H), 6.97 (d, *J* = 8.8 Hz, 2H), 7.14 (d, *J* = 8.8 Hz, 2H).

3-(4-(4-(4-(Cyclopropanecarbonyl)piperazin-1-yl)butoxy)phenyl)thiazolidine-2,4-dione (12d). Yield: 59%, ^{1}H NMR (400 MHz, $CDCl_3$) δ: 0.74–0.77 (m, 2H), 0.96−0.99 (m, 2H), 1.66–1.76 (m, 3H), 1.86–1.89 (m, 2H), 2.40–2.50 (m, 6H), 3.64–3.68 (m, 4H), 4.00 (t, *J* = 6.2

Hz, 2H), 4.10 (s, 2H), 6.97 (d, *J* = 8.8 Hz, 2H), 7.14 (d, *J* = 8.8 Hz, 2H).

3-(4-(4-(4-(Cyclopropylmethyl)piperazin-1-yl)butoxy)phenyl)thiazolidine-2,4-dione (12e). Yield: 41%, ^{1}H NMR (400 MHz, $CDCl_3$) δ: 0.09–0.10 (m, 2H), 0.48–0.50 (m, 2H), 0.80–1.00 (m, 1H), 1.60–1.70 (m, 2H), 1.75–1.85 (m, 2H), 2.19 (d, *J* = 6.5 Hz, 2H), 2.34–2.43 (m, 10H), 4.07 (t, *J* = 6.4 Hz, 2H), 4.33 (s, 2H), 6.97 (d, *J* = 8.8 Hz, 2H), 7.14 (d, *J* = 8.8 Hz, 2H).

3-(4-(3-(4-(Cyclopropylmethyl)piperazin-1-yl)propoxy)phenyl)thiazolidine-2,4-dione (12f). Yield: 38%, ^{1}H NMR (400 MHz, $CDCl_3$) δ: 0.03–0.07 (m, 2H), 0.46–0.48 (m, 2H), 0.83 (s, 1H), 1.92–1.95 (m, 2H), 2.22–2.50 (m, 12H), 3.99 (t, *J* = 6.4 Hz, 2H), 4.04 (s, 2H), 6.97 (d, *J* = 8.8 Hz, 2H), 7.14 (d, *J* = 8.8 Hz, 2H).

3-(4-(5-(4-(Cyclopropylmethyl)piperazin-1-yl)pentyloxy)phenyl)thiazolidine-2,4-dione (12g). Yield: 48% ^{1}H NMR (400 MHz, $CDCl_3$) δ: 0.06–0.07 (m, 2H), 0.46–0.48 (m, 2H), 0.83 (s, 1H), 1.44–1.45 (m, 2H), 1.52–1.53 (m, 2H), 1.76–1.79 (m, 2H), 2.22–2.49 (m, 12H), 3.93 (t, *J* = 6.4 Hz, 2H), 4.04 (s, 2H), 6.97 (d, *J* = 8.8 Hz, 2H), 7.14 (d, *J* = 8.8 Hz, 2H).

General procedure of the target compounds (6a–x). Sodium acetate anhydrous (17.6 mg, 0.21 mmol), the appropriate aldehyde derivative (0.14 mmol) and the appropriate 3-(4-(*N*-(4-substitutedpiperazin-1-yl)alkoxy)phenyl)thiazolidine-2,4-dione (**12**, 0.07 mmol) were dissolved in acetic acid (3 mL) and stirred at 110 ^{o}C for 16 h. After cooling, the mixture was neutralized to pH 8 by addition of ammonium hydroxide and extracted with DCM. The organic layer was dried over anhydrous $MgSO_4$, filtered and concentrated under reduced pressure. The residue was purified by column chromatography (SiO_2, DCM/MeOH 15:1 v/v

including 1% of ammonium hydroxide).

(Z)-3-(4-(4-(4-(Methylsulfonyl)piperazin-1-yl)butoxy)phenyl)-5-(4-(4-nitrophenoxy)benzylidene)thiazolidine-2,4-dione (6a). Yield: 21%, HPLC purity: 9.23 min, 97.70%, ^{1}H NMR (400 MHz, $CDCl_3$) δ: 1.66–1.70 (m, 2H), 1.80–1.86 (m, 2H), 2.46 (t, *J* = 7.1 Hz, 2H), 2.55–2.57 (m, 4H), 2.77 (s, 3H), 3.23–3.24 (m, 4H), 4.03 (t, *J* = 6.1 Hz, 2H), 7.00 (d, *J* = 8.8 Hz, 2H), 7.12 (d, *J* = 9.0 Hz, 2H), 7.20 (d, *J* = 8.5 Hz, 2H), 7.24 (d, *J* = 8.8 Hz, 2H), 7.61 (d, *J* = 8.6 Hz, 2H), 7.96 (s, 1H), 8.27 (d, *J* = 9.1 Hz, 2H). HRMS (ES+): *m/z* calculated for $C_{31}H_{32}N_4O_8S_2$: 653.1740 $[M+H]^+$. Found 653.1733, 675.1560 $[M+Na]^+$. Found 675.1541.

(Z)-5-(4-(4-Fluorophenoxy)benzylidene)-3-(4-(4-(4-(methylsulfonyl)piperazin-1-yl)butoxy)phenyl)thiazolidine-2,4-dione (6b). Yield: 12%, HPLC purity: 6.36 min, 100%, ^{1}H NMR (400 MHz, $CDCl_3$) δ: 1.66–1.69 (m, 2H), 1.81–1.85 (m, 2H), 2.46 (t, *J* = 7.1 Hz, 2H), 2.56–2.57 (m, 4H), 2.77 (s, 3H), 3.23–3.25 (m, 4H), 4.02 (t, *J* = 6.1 Hz, 2H), 6.98–7.12 (m, 8H), 7.23 (d, *J* = 8.9 Hz, 2H), 7.51 (d, *J* = 8.8 Hz, 2H), 7.93 (s, 1H). HRMS (ES+): *m/z* calculated for $C_{31}H_{32}FN_3O_6S_2$: 626.1795 $[M+H]^+$. Found 626.1795.

(Z)-5-(4-(4-Chlorophenoxy)benzylidene)-3-(4-(4-(4-(methylsulfonyl)piperazin-1-yl)butoxy)phenyl)thiazolidine-2,4-dione (6c). Yield: 14%, HPLC purity: 6.59 min, 100%, ^{1}H NMR (400 MHz, $CDCl_3$) δ: 1.66–1.72 (m, 2H), 1.80–1.85 (m, 2H), 2.46 (t, *J* = 7.1 Hz, 2H), 2.56–2.57 (m, 4H), 2.77 (s, 3H), 3.23–3.25 (m, 4H), 4.02 (t, *J* = 6.1 Hz, 2H), 6.98–7.03 (m, 4H), 7.06 (d, *J* = 8.6 Hz, 2H), 7.23 (d, *J* = 8.8 Hz, 2H), 7.36 (d, *J* = 8.7 Hz, 2H), 7.52 (d, *J* = 8.6 Hz, 2H), 7.94 (s, 1H). HRMS (ES+): *m/z* calculated for $C_{31}H_{32}ClN_3O_6S_2$: 642.1499

$[M+H]^+$. Found 642.1508.

(Z)-5-(4-(4-Bromophenoxy)benzylidene)-3-(4-(4-(4-(methylsulfonyl)piperazin-1-yl)butoxy)phenyl)thiazolidine-2,4-dione (6d). Yield: 13%, HPLC purity: 9.56 min, 97.16%, ^{1}H NMR (400 MHz, $CDCl_3$) δ: 1.57–1.61 (m, 2H), 1.74–1.77 (m, 2H), 2.38 (t, *J* = 6.9 Hz, 2H), 2.45–2.46 (m, 4H), 2.85 (s, 3H), 3.08–3.10 (m, 4H), 4.04 (t, *J* = 6.4 Hz, 2H), 7.06 (d, *J* = 8.7 Hz, 2H), 7.11 (d, *J* = 8.6 Hz, 2H), 7.18 (*J* = 8.7 Hz, 2H), 7.33 (d, *J* = 8.7 Hz, 2H), 7.63 (d, *J* = 8.7 Hz, 2H), 7.71 (d, *J* = 8.7 Hz, 2H), 7.96 (s, 1H). HRMS (ES+): *m/z* calculated for $C_{31}H_{32}BrN_3O_6S_2$: 686.0994 $[M+H]^+$. Found 686.0967, 708.0814 $[M+Na]^+$. Found 708.0772.

(Z)-3-(4-(4-(4-(2-Methoxyethyl)piperazin-1-yl)butoxy)phenyl)-5-(4-(4-nitrophenoxy)benzylidene)thiazolidine-2,4-dione (6e). Yield: 12%, ^{1}H NMR (400 MHz, $CDCl_3$) δ: 1.65–1.69 (m, 2H), 1.79–1.84 (m, 2H), 2.41 (t, *J* = 7.4 Hz, 2H), 2.53–2.60 (m, 10H), 3.35 (s, 3H), 3.51 (t, *J* = 5.6 Hz, 2H), 4.01 (t, *J* = 6.2 Hz, 2H), 6.99–7.01 (m, *J* = 8.9 Hz, 2H), 7.13 (d, *J* = 9.1 Hz, 2H), 7.19 (d, *J* = 8.7 Hz, 2H), 7.23 (d, *J* = 8.9 Hz, 2H), 7.61 (d, *J* = 8.7 Hz, 2H), 7.96 (s, 1H), 8.26 (d, *J* = 9.1 Hz, 2H). HRMS (ES+): *m/z* calculated for $C_{33}H_{36}N_4O_7S$: 633.2383 $[M+H]^+$. Found 633.2391.

(Z)-5-(4-(4-Fluorophenoxy)benzylidene)-3-(4-(4-(4-(2-methoxyethyl)piperazin-1-yl)butoxy)phenyl)thiazolidine-2,4-dione (6f). Yield: 54%, HPLC purity: 6.37 min, 100%, ^{1}H NMR (400 MHz, $CDCl_3$) δ: 1.65–1.68 (m, 2H), 1.80–1.83 (m, 2H), 2.40 (t, *J* = 7.4 Hz, 2H), 2.52–2.59 (m, 10H), 3.34 (s, 3H), 3.51 (t, *J* = 5.6 Hz, 2H), 4.00 (t, *J* = 6.2 Hz, 2H), 6.98–7.12 (m, 8H), 7.21 (d, *J* = 8.8 Hz, 2H), 7.50 (d, *J* = 8.7 Hz, 2H), 7.93 (s, 1H). ^{13}C NMR (100.6 MHz, $CDCl_3$) δ: 23.4, 27.2, 53.0, 53.5, 57.9, 58.1, 58.9, 68.0, 70.1, 115.2, 116.6, 116.9, 117.9, 119.4, 121.7, 121.8, 125.0, 127.8, 128.5, 132.3, 133.6, 151.2, 159.5, 160.1, 166.7 ($J_{C\text{-}F}$

= 145.8 Hz). HRMS (ES+): *m/z* calculated for $C_{33}H_{36}FN_3O_5S$: 606.2438 $[M+H]^+$. Found 606.2360.

(Z)-5-(4-(4-Chlorophenoxy)benzylidene)-3-(4-(4-(4-(2-methoxyethyl)piperazin-1-yl)butoxy)phenyl)thiazolidine-2,4-dione (6g). Yield: 30%, HPLC purity: 6.61 min, 100%, ^{1}H NMR (400 MHz, $CDCl_3$) δ: 1.65–1.69 (m, 2H), 1.78–1.83 (m, 2H), 2.39–2.60 (m, 12H), 3.35 (s, 3H), 3.51 (t, *J* = 5.6 Hz, 2H), 4.00 (t, *J* = 6.2 Hz, 2H), 6.95–7.07 (m, 6H), 7.22 (d, *J* = 8.8 Hz, 2H), 7.36 (d, *J* = 8.7 Hz, 2H), 7.52 (d, *J* = 8.7 Hz, 2H), 7.94 (s, 1H). ^{13}C NMR (100.6 MHz, $CDCl_3$) δ: 23.3, 27.2, 53.0, 53.5, 57.9, 58.1, 58.9, 68.0, 70.1, 115.3, 118.5, 119.7, 121.3, 125.0, 128.2, 128.4, 129.8, 130.1, 132.3, 133.5, 154.2, 159.4, 159.5, 166.1, 167.6. HRMS (ES+): *m/z* calculated for $C_{33}H_{36}ClN_3O_5S$: 622.2142 $[M+H]^+$. Found 622.2145.

(Z)-5-(4-(4-Bromophenoxy)benzylidene)-3-(4-(4-(4-(2-methoxyethyl)piperazin-1-yl)butoxy)phenyl)thiazolidine-2,4-dione (6h). Yield: 9%, HPLC purity: 9.10 min, 94.28%, ^{1}H NMR (400 MHz, $CDCl_3$) δ: 1.64–1.65 (m, 2H), 1.72–1.77 (m, 2H), 2.42–2.57 (m, 12H), 3.27 (s, 3H), 3.46 (t, *J* = 5.4 Hz, 2H), 3.93 (t, *J* = 6.0 Hz, 2H), 6.88–6.93 (m, 4H), 6.99 (d, *J* = 8.6 Hz, 2H), 7.15 (d, *J* = 8.8 Hz, 2H), 7.42–7.46 (m, 4H), 7.86 (s, 1H). HRMS (ES+): *m/z* calculated for $C_{33}H_{36}BrN_3O_5S$: 666.1637 $[M+H]^+$. Found 666.1656.

(Z)-3-(4-(4-(4-(3-Methoxypropyl)piperazin-1-yl)butoxy)phenyl)-5-(4-(4-nitrophenoxy)benzylidene)thiazolidine-2,4-dione (6i). Yield: 16%, ^{1}H NMR (400 MHz, $CDCl_3$) δ: 1.66–1.70 (m, 2H), 1.76–1.84 (m, 4H), 2.40–2.52 (m, 12H), 3.32 (s, 3H), 3.42 (t, *J* = 6.4 Hz, 2H), 4.01 (t, *J* = 6.2 Hz, 2H), 7.00 (d, *J* = 8.8 Hz, 2H), 7.12 (d, *J* = 9.1 Hz, 2H), 7.19 (d, *J* = 8.6 Hz, 2H), 7.23 (d, *J* = 8.9 Hz, 2H), 7.61 (d, *J* = 8.6 Hz, 2H), 7.96 (s, 1H), 8.26 (d, *J* = 9.1 Hz, 2H).

(Z)-5-(4-(4-Fluorophenoxy)benzylidene)-3-(4-(4-(4-(3-methoxypropyl)piperazin-1-yl)butoxy)phenyl)thiazolidine-2,4-dione (6j). Yield: 24%, ^{1}H NMR (400 MHz, $CDCl_3$) δ: 1.67–1.71 (m, 2H), 1.73–1.83 (m, 4H), 2.38–2.49 (m, 12H), 3.32 (s, 3H), 3.41 (t, *J* = 6.3 Hz, 2H), 4.00 (t, *J* = 6.1 Hz, 2H), 6.98–7.12 (m, 8H), 7.22 (d, *J* = 8.7 Hz, 2H), 7.50 (d, *J* = 8.6 Hz, 2H), 7.93 (s, 1H).

(Z)-5-(4-(4-Chlorophenoxy)benzylidene)-3-(4-(4-(4-(3-methoxypropyl)piperazin-1-yl)butoxy)phenyl)thiazolidine-2,4-dione (6k). Yield: 19%, HPLC purity: 6.62 min, 100%, ^{1}H NMR (400 MHz, $CDCl_3$) δ: 1.65–1.71 (m, 2H), 1.74–1.85 (m, 4H), 2.39–2.50 (m, 12H), 3.32 (s, 3H), 3.41 (t, *J* = 6.4 Hz, 2H), 4.00 (t, *J* = 6.2 Hz, 2H), 6.98–7.07 (m, 6H), 7.22 (d, *J* = 8.8 Hz, 2H), 7.34 (d, *J* = 8.8 Hz, 2H), 7.40 (d, *J* = 8.7 Hz, 2H), 7.93 (s, 1H). HRMS (ES+): *m/z* calculated for $C_{34}H_{38}ClN_3O_5S$: 636.2299 $[M+H]^+$. Found 636.2301.

(Z)-5-(4-(4-Bromophenoxy)benzylidene)-3-(4-(4-(4-(3-methoxypropyl)piperazin-1-yl)butoxy)phenyl)thiazolidine-2,4-dione (6l). Yield: 4%, HPLC purity: 6.68 min, 100%, ^{1}H NMR (400 MHz, $CDCl_3$) δ: 1.67–1.69 (m, 2H), 1.75–1.83 (m, 4H), 2.39–2.49 (m, 12H), 3.32 (s, 3H), 3.41 (t, *J* = 6.4 Hz, 2H), 4.01 (t, *J* = 6.2 Hz, 2H), 6.96–7.01 (m, 4H), 7.07 (d, *J* = 8.7 Hz, 2H), 7.22 (d, *J* = 8.8 Hz, 2H), 7.49–7.53 (m, 4H), 7.94 (s, 1H). HRMS (ES+): *m/z* calculated for $C_{34}H_{38}BrN_3O_5S$: 680.1794 $[M+H]^+$. Found 680.1796.

(Z)-3-(4-(4-(4-(Cyclopropanecarbonyl)piperazin-1-yl)butoxy)phenyl)-5-(4-(4-nitrophenoxy)benzylidene)thiazolidine-2,4-dione (6m). Yield: 5%, ^{1}H NMR (400 MHz, $CDCl_3$) δ: 0.73–0.78 (m, 2H), 0.97–1.00 (m, 2H), 1.68–1.75 (m, 3H), 1.81–1.86 (m, 2H), 2.42–2.49 (m, 6H), 3.65–3.69 (m, 4H), 4.03 (t, *J* = 6.1 Hz, 2H), 7.01 (d, *J* = 8.9 Hz, 2H), 7.12

(d, *J* = 9.1 Hz, 2H), 7.19 (d, *J* = 8.6 Hz, 2H), 7.23 (d, *J* = 8.8 Hz, 2H), 7.61 (d, *J* = 8.6 Hz, 2H), 7.96 (s, 1H), 8.26 (d, *J* = 9.1 Hz, 2H). HRMS (ES+): *m/z* calculated for $C_{34}H_{34}N_4O_7S$: 643.2226 $[M+H]^+$. Found 643.2232, 665.2046 $[M+Na]^+$. Found 665.2050.

(Z)-3-(4-(4-(4-(Cyclopropanecarbonyl)piperazin-1-yl)butoxy)phenyl)-5-(4-(4-fluorophenoxy)benzylidene)thiazolidine-2,4-dione (6n). Yield: 6%, ^{1}H NMR (400 MHz, $CDCl_3$) δ: 0.73–0.77 (m, 2H), 0.97–0.99 (m, 2H), 1.66–1.74 (m, 3H), 2.40–2.54 (m, 6H), 3.65–3.69 (m, 4H), 4.01 (t, *J* = 6.2 Hz, 2H), 6.98– 7.12 (m, 8H), 7.22 (d, *J* = 8.9 Hz, 2H), 7.51 (d, *J* = 8.7 Hz, 2H), 7.93 (s, 1H). HRMS (ES+): *m/z* calculated for $C_{34}H_{34}FN_3O_5S$: 616.2281 $[M+H]^+$. Found 616.2279.

(Z)-5-(4-(4-Chlorophenoxy)benzylidene)-3-(4-(4-(4-(cyclopropanecarbonyl)piperazin-1-yl)butoxy)phenyl)thiazolidine-2,4-dione (6o). Yield: 23%, HPLC purity: 6.59 min, 100%, ^{1}H NMR (400 MHz, $CDCl_3$) δ: 0.74–0.77 (m, 2H), 0.96–1.00 (m, 2H), 1.67–1.75 (m, 3H), 1.82–1.86 (m, 2H), 2.41–2.48 (m, 6H), 3.65–3.68 (m, 4H), 4.02 (t, *J* = 6.2 Hz, 2H), 6.99–7.04 (m, 4H), 7.06 (d, *J* = 8.7 Hz, 2H), 7.23 (d, *J* = 8.9 Hz, 2H), 7.36 (d, *J* = 8.8 Hz, 2H), 7.52 (d, *J* = 8.7 Hz, 2H), 7.93 (s, 1H). HRMS (ES+): *m/z* calculated for $C_{34}H_{34}ClN_3O_5S$: 632.1986 $[M+H]^+$. Found 632.1982.

(Z)-5-(4-(4-Bromophenoxy)benzylidene)-3-(4-(4-(4-(cyclopropanecarbonyl)piperazin-1-yl)butoxy)phenyl)thiazolidine-2,4-dione (6p). Yield: 14%, ^{1}H NMR (400 MHz, $CDCl_3$) δ: 0.74–0.77 (m, 2H), 0.97–0.98 (m, 2H), 1.67–1.75 (m, 3H), 1.82–1.86 (m, 2H), 2.42–2.48 (m, 6H), 3.65–3.68 (m, 4H), 4.02 (t, *J* = 5.9 Hz, 2H), 6.97 (d, *J* = 8.7 Hz, 2H), 7.00 (d, *J* = 8.8 Hz, 2H), 7.07 (d, *J* = 8.4 Hz, 2H), 7.23 (d, *J* = 8.6 Hz, 2H), 7.49–7.53 (m, 4H), 7.93 (s, 1H). HRMS (ES+): *m/z* calculated for $C_{34}H_{34}BrN_3O_5S$: 676.1481 $[M+H]^+$. Found 676.1486.

(Z)-3-(4-(4-(4-(Cyclopropylmethyl)piperazin-1-yl)butoxy)phenyl)-5-(4-(4-nitrophenoxy)benzylidene)thiazolidine-2,4-dione (6q). Yield: 4%, ^{1}H NMR (400 MHz, $CDCl_3$) δ: 0.10–0.11 (m, 2H), 0.50–0.52 (m, 2H), 1.68–1.71 (m, 3H), 1.81–1.84 (m, 2H), 2.26 (d, *J* = 6.5 Hz, 2H), 2.41–2.54 (m, 10H), 4.01 (t, *J* = 6.2 Hz, 2H), 7.01 (d, *J* = 8.9 Hz, 2H), 7.12 (d, *J* = 9.1 Hz, 2H), 7.19 (d, *J* = 8.6 Hz, 2H), 7.23 (d, *J* = 8.8 Hz, 2H), 7.61 (d, *J* = 8.7 Hz, 2H), 7.97 (s, 1H), 8.27 (d, *J* = 9.1 Hz, 2H). HRMS (ES+): *m/z* calculated for $C_{34}H_{36}N_4O_6S$: 629.2434 $[M+H]^+$. Found 629.2445.

(Z)-3-(4-(4-(4-(Cyclopropylmethyl)piperazin-1-yl)butoxy)phenyl)-5-(4-(4-fluorophenoxy)benzylidene)thiazolidine-2,4-dione (6r). Yield: 18%, HPLC purity: 6.46 min, 100%, ^{1}H NMR (400 MHz, $CDCl_3$) δ: 0.08–0.10 (m, 2H), 0.48–0.50 (m, 2H), 0.85–0.88 (m, 1H), 1.64–1.68 (m, 2H), 1.79–1.82 (m, 2H), 2.25 (d, *J* = 6.5 Hz, 2H), 2.38–2.52 (m, 10H), 3.99 (t, *J* = 6.2 Hz, 2H), 6.97– 7.10 (m, 8H), 7.20 (d, *J* = 8.9 Hz, 2H), 7.48 (d, *J* = 8.8 Hz, 2H), 7.91 (s, 1H). HRMS (ES+): *m/z* calculated for $C_{34}H_{36}FN_3O_4S$: 602.2489 $[M+H]^+$. Found 602.2490.

(Z)-5-(4-(4-Chlorophenoxy)benzylidene)-3-(4-(4-(4-(cyclopropylmethyl)piperazin-1-yl)butoxy)phenyl)thiazolidine-2,4-dione (6s). Yield: 29%, HPLC purity: 6.64 min, 100%, ^{1}H NMR (400 MHz, $CDCl_3$) δ: 0.09–0.12 (m, 2H), 0.48–0.53 (m, 2H), 0.87–0.88 (m, 1H), 1.66–1.71 (m, 2H), 1.79–1.84 (m, 2H), 2.26 (d, *J* = 6.5 Hz, 2H), 2.40–2.60 (m, 10H), 4.01 (t, *J* = 6.2 Hz, 2H), 6.99–7.07 (m, 6H), 7.22 (d, *J* = 8.9 Hz, 2H), 7.36 (d, *J* = 8.8 Hz, 2H), 7.52 (d, *J* = 8.7 Hz, 2H), 7.94 (s, 1H). HRMS (ES+): *m/z* calculated for $C_{34}H_{36}ClN_3O_4S$: 618.2193 $[M+H]^+$. Found 618.2196.

(Z)-5-(4-(4-Bromophenoxy)benzylidene)-3-(4-(4-(4-(cyclopropylmethyl)piperazin-1-yl)butoxy)phenyl)thiazolidine-2,4-dione (6t). Yield: 7%, ^{1}H NMR (400 MHz, $CDCl_3$) δ: 0.07–0.10 (m, 2H), 0.50–0.52 (m, 2H), 0.87–0.88 (m, 1H), 1.68–1.71 (m, 2H), 1.81–1.82 (m, 2H), 2.26 (d, *J* = 6.3 Hz, 2H), 2.40–2.53 (m, 10H), 4.01 (t, *J* = 6.2 Hz, 2H), 6.95–7.01 (m, 4H), 7.07 (d, *J* = 8.6 Hz, 2H), 7.22 (d, *J* = 8.7 Hz, 2H), 7.49–7.53 (m, 4H), 7.93 (s, 1H). HRMS (ES+): *m/z* calculated for $C_{34}H_{36}BrN_3O_4S$: 662.1688 $[M+H]^+$. Found 662.1689.

(Z)-3-(4-(3-(4-(Cyclopropylmethyl)piperazin-1-yl)propoxy)phenyl)-5-(4-(4-fluorophenoxy)benzylidene)thiazolidine-2,4-dione (6u). Yield: 13%, HPLC purity: 6.43 min, 92.78%, ^{1}H NMR (400 MHz, $CDCl_3$) δ: 0.09–0.12 (m, 2H), 0.49–0.53 (m, 2H), 0.84–0.89 (m, 1H), 1.95–2.04 (m, 2H), 2.27 (d, *J* = 6.5 Hz, 2H), 2.51–2.55 (m, 10H), 4.05 (t, *J* = 6.2 Hz, 2H), 6.97–7.13 (m, 8H), 7.22 (d, *J* = 8.9 Hz, 2H), 7.51 (d, *J* = 8.7 Hz, 2H), 7.93 (s, 1H). HRMS (ES+): *m/z* calculated for $C_{33}H_{34}FN_3O_4S$: 588.2332 $[M+H]^+$. Found 588.2333.

(Z)-3-(4-(5-(4-(Cyclopropylmethyl)piperazin-1-yl)pentyloxy)phenyl)-5-(4-(4-fluorophenoxy)benzylidene)thiazolidine-2,4-dione (6v). Yield: 13%, HPLC purity: 6.53 min, 100%, ^{1}H NMR (400 MHz, $CDCl_3$) δ: 0.07–0.10 (m, 2H), 0.48–0.51 (m, 2H), 0.85–0.88 (m, 1H), 1.48–1.61 (m, 4H), 1.78–1.85 (m, 2H), 2.26 (d, *J* = 6.5 Hz, 2H), 2.36–2.53 (m, 10H), 3.98 (t, *J* = 6.2 Hz, 2H), 6.98–7.12 (m, 8H), 7.22 (d, *J* = 8.8 Hz, 2H), 7.51 (d, *J* = 8.6 Hz, 2H), 7.93 (s, 1H). HRMS (ES+): *m/z* calculated for $C_{35}H_{38}FN_3O_4S$: 616.2645 $[M+H]^+$. Found 616.2646.

(Z)-5-(3-Chloro-4-morpholinobenzylidene)-3-(4-(3-(4-(cyclopropylmethyl)piperazin-1-yl)propoxy)phenyl)thiazolidine-2,4-dione (6w)

Yield: 12%, HPLC purity: 6.09 min, 100%, ^{1}H NMR (400 MHz, $CDCl_3$) δ: 0.08–0.12 (m, 2H), 0.49–0.53 (m, 2H), 0.84–0.89 (m, 1H), 1.95–2.04 (m, 2H), 2.27 (d, *J* = 6.5 Hz, 2H), 2.51–2.55 (m, 10H), 3.15–3.17 (m, 4H), 3.88–3.90 (m, 4H), 4.04 (t, *J* = 6.2 Hz, 2H), 7.00 (d, *J* = 8.9 Hz, 1H), 7.10 (d, *J* = 8.4 Hz, 2H), 7.21 (d, *J* = 8.8 Hz, 2H), 7.43 (dd, *J* = 2.0, 8.4 Hz, 1H), 7.55 (d, *J* = 2.0 Hz, 1H), 7.84 (s, 1H). HRMS (ES+): *m/z* calculated for $C_{31}H_{37}ClN_4O_4S$: 597.2302 $[M+H]^+$. Found 597.2308.

(Z)-5-(3-Chloro-4-morpholinobenzylidene)-3-(4-((5-(4-(cyclopropylmethyl)piperazin-1-yl)pentyl)oxy)phenyl)thiazolidine-2,4-dione (6x)

Yield: 17%, HPLC purity: 6.27 min, 100%, ^{1}H NMR (400 MHz, $CDCl_3$) δ: 0.08–0.11 (m, 2H), 0.48–0.52 (m, 2H), 0.85–0.88 (m, 1H), 1.47–1.61 (m, 4H), 1.78–1.85 (m, 2H), 2.26 (d, *J* = 6.5 Hz, 2H), 2.35–2.53 (m, 10H), 3.15–3.17 (m, 4H), 3.85–3.90 (m, 4H), 3.98 (t, *J* = 6.3 Hz, 2H), 6.99 (d, *J* = 8.8 Hz, 1H), 7.10 (d, *J* = 8.4 Hz, 2H), 7.21 (d, *J* = 8.8 Hz, 2H), 7.43 (dd, *J* = 1.9, 8.4 Hz, 1H), 7.55 (d, *J* = 1.9 Hz, 1H), 7.84 (s, 1H). HRMS (ES+): *m/z* calculated for $C_{33}H_{41}ClN_4O_4S$: 625.2615 $[M+H]^+$. Found 625.2620.

4.2. *In vitro* IMAP® TR-FRET assay of IKK-β

IKK2 kinase reactions were performed in a reaction buffer (10 mM Tris–HCl, pH 7.2, 10 mM $MgCl_2$, 0.05% NaN_3) containing 1 mM DTT and 0.01% Tween-20 (Sigma-Aldrich) to stabilize the enzyme. The reactions were performed at room temperature for 2 h in white standard 384 plates (3572, Corning Life Sciences, Lowell, MA, USA) using 0.5 μg/mL IKK2 (Millipore Co., Billerica, MA, USA), 1 μM IκBα-derived substrate (5FAMGRHDSGLDSMK-NH_2; R7574, MDS Analytical Technologies, Ontario, Canada), and 3 μM ATP (Sigma-Aldrich). The total reaction volumes were 20 μL, and 10 μM compounds were pre-incubated with IKK2 enzyme for 10 min before the substrate and ATP

were added. For the TR-FRET reaction, 60 µL detection mixture, 1:600 dilution of IMAP binding reagent and 1:400 dilution of Terbium donor supplied by MDS Analytical Technologies, was added 15 h before reading the plate. The energy transfer signal was measured in a multi-label counter using the TR-FRET option (Victor II, PerkinElmer Oy, Turku, Finland). The counter setting was 340 nm excitation, 100-µs delay, and dual-emission collection for 200 µs at 495 and 520 nm. The energy transfer signal data were used to calculate the percentage inhibition and IC_{50} values. The kinetic study was conducted as mentioned above using ten doses (30, 10, 3, 1, 0.3, 0.1, 0.03, 0.01, 0.003 and 0.001 µM concentrations) of the tested compounds. However, the reactions were performed for 0, 20, 40 and 60 minutes instead of the 2 h reaction.

4.3. *In vitro* cell-based assay

4.3.1. Cell culture

RAW 264.7 macrophage cells were obtained from the Korean Cell Line Bank (Seoul, Republic of Korea). Dulbecco's modified eagle's medium (DMEM), fetal bovine serum, penicillin, and streptomycin were obtained from Life Technologies Inc. (Grand Island, NY, USA). The Raw 264.7 macrophage cells were grown at 37 °C in DMEM containing 10% fetal bovine serum, penicillin (100 units/ml) and streptomycin sulfate (100 µg/ml) in a 5% CO_2 atmosphere.

4.3.2. Cell viability

RAW 264.7 macrophage cells were seeded at 1×10^5 cells/mL in 96-well plates containing 100 µL of DMEM medium with 10% FBS and incubated overnight. After overnight incubation, tested samples were added and the plates were incubated for 24 h. The cells were then incubated with a MTT solution [(3-(4,5-dimethylthiazol-2-yl)-2,5-diphenyltetrazolium

bromide, 5 mg/mL stock solution in PBS] for 4 h at 37 °C under 5% CO_2. The medium was discarded and the formazan blue that formed in the cells was dissolved in 200 μL DMSO. Absorbance of each well was measured at 540 nm using a microplate reader (Molecular Devices Inc., CA, USA).

4.3.3. PGE_2 and TNF-α assays

Cells were plated at 2×10^5 cells/mL (RAW 264.7 macrophages) in 24-well plates and incubated overnight. Following treatment with various concentrations of samples at various concentrations or with an NS-398 (positive control) for 1 h, cells were treated with LPS (10 ng/mL) for 24 h. Dilutions of the cell culture medium were assayed for PGE_2 and TNF-α levels using a colorimetric competitive enzyme-linked immunosorbent assay (ELISA) kit (Enzo life science, NY, USA) according to the manufacturer's instructions. TNF-α and PGE_2 levels in cell culture medium were quantified by ELISA using mouse DuoSet kit (R&D Systems, MN, USA) according to the manufacturer's instructions.

4.4. Assay of hERG inhibition

4.4.1. Cell culture and preparation

CHO-K1 cells expressing hERG channels (CHO-K1 Tet-On hERG cells) were purchased (IonGate Biosciences GmbH, Frankfurt, Germany). Cells were cultured in Dulbecco's modified Eagle's medium containing 10% (vol./vol.) fetal bovine serum, penicillin (100 U/ml), streptomycin (100 μg/ml), fungizone (2.5 μg/ml), geneticin G418 (200 μg/ml), hygromycin (200 μg/ml), and puromycin (2 μg/ml) in humidified 5% CO_2 at 37 °C. hERG channel expression induced by 5 μg/ml of doxycyclin (Sigma, St. Louis, MO, USA). Cells were prepared for automated patch-clamp recordings by plating into the 100 mm culture dishes, harvesting with trypsin–EDTA when cells have 50%–80% confluency, washing twice,

and resuspension in the extracellular to 1–5 × 10^6 cells per milliliter. Cells were used for recordings 20–32 h after doxycycline treatment.

4.4.2. Automated patch-clamp electrophysiology assay of hERG inhibition

NPC-16 Patchliner (Nanion Technologies, München, Germany) was used for whole-cell recordings with the intracellular solution containing (in mM) 50 KCl, 60 KF, 10 NaCl, 2 $MgCl_2$, 20 EGTA, and 10 HEPES (pH 7.2), and with the extracellular solution containing (in mM) 140 NaCl, 4 KCl, 2 $CaCl_2$, 1 $MgCl_2$, 5 glucose, and 10 HEPES (pH 7.4). For stable seal formation, the seal enhancer containing (in mM) 80 NaCl, 3 KCl, 35 $CaCl_2$, 10 $MgCl_2$, and 10 HEPES (pH 7.4) was used at the seal formation step. Before the whole-cell recordings, the external seal enhancing solution was exchanged to the extracellular solution. hERG channel currents were recorded using the parallel EPC-10 patch-clamp amplifiers (HEKA Elektronik, Lambrecht/Pfalz, Germany) and low-pass filtered (10 kHz) with a 4-pole Bessel filter. Cell suspension and patch solutions were automatically added onto the four recording wells in the microfabricated disposable chip (NPC-16 Chip, Nanion Technologies, München, Germany). To obtain the inhibitory constants, hERG tail currents were evoked by repolarizing steps to −50 mV for 500 ms preceded by a 500 ms depolarization potential of +20 mV at a holding potential of −80 mV with a 20 s sweep interval. To measure the inactivation rates, re-inactivating hERG channel currents were elicited on return to +20 mV after a 30 ms pulse to −80 mV at a holding potential of +20 mV in the absence and presence of each QA. Whole-cell currents were acquired and digitized at 5 kHz, and linear leak currents were subtracted employing a standard P/−4 leak subtraction protocol using the Patchmaster (HEKA Elektronik, Lambrecht/Pfalz, Germany). Both raw and leak subtracted data were recorded. The extracellular solution was exchanged to the extracellular solution containing each tested compound T *via* 4 pipette tips of NPC-16 Patchliner using a 4-fold volume of solution (40 μl)

with a speed of 4 μl/s, and the exchanged tested compound solution was applied for 100–200 s to the patch-clamped cells until compound binding had reached equilibrium (monitoring hERG tail currents).

Whole-cell recordings were analyzed using the Patchmaster/Fitmaster (HEKA Elektronik, Lambrecht/Pfalz, Germany), IGOR Pro (WaveMetrics Inc., Portland, OR, USA), and the GraphPad Prism 4 (GraphPad Software, Inc., La Jolla, CA, USA) software. The percent inhibition was calculated as:

% Inhibition = $(I_{CTR} - I_T) / I_{CTR}$, where I_{CTR} and I_T are the amplitude of hERG tail current before and after the application of T, respectively.

To yield concentration–response curves, the concentration–response data were fitted with a Hill equation,

% Inhibition = $100 / (1 + (K_i / [T])^h)$, where K_i is the inhibitory constant, [T] is concentration of test compound, and h is the Hill coefficient.

5. Conflict of Interest

Authors declare no conflict of interest.

6. Acknowledgement

This work was supported by the KIST Institutional programs (Grant No. 2E28010) from Korea Institute of Science and Technology and by the Creative Fusion Research Program through the Creative Allied Project funded by the National Research Council of Science & Technology (CAP-12-1-KIST).

References

[1] M.E. Swarbrick, Chapter 3 The Learning and Evolution of Medicinal Chemistry against Kinase

Targets, in: Kinase Drug Discovery, The Royal Society of Chemistry, 2012, pp. 79-95.
[2] P. Cohen, The regulation of protein function by multisite phosphorylation – a 25 year update, Trends in Biochemical Sciences, 25 (2000) 596-601.
[3] D. Huang, T. Zhou, K. Lafleur, C. Nevado, A. Caflisch, Kinase selectivity potential for inhibitors targeting the ATP binding site: a network analysis, Bioinformatics, 26 (2010) 198-204.
[4] Z. Fang, C. Grutter, D. Rauh, Strategies for the selective regulation of kinases with allosteric modulators: exploiting exclusive structural features, ACS chemical biology, 8 (2013) 58-70.
[5] S. Muller, S. Knapp, CHAPTER 3 Targeting Catalytic and Non-Catalytic Functions of Protein Kinases, in: Allosterism in Drug Discovery, The Royal Society of Chemistry, 2017, pp. 40-64.
[6] J.A. Schmid, A. Birbach, IkappaB kinase beta (IKKbeta/IKK2/IKBKB)--a key molecule in signaling to the transcription factor NF-kappaB, Cytokine & growth factor reviews, 19 (2008) 157-165.
[7] D.S. Straus, Design of small molecules targeting transcriptional activation by NF-κB: overview of recent advances, Expert Opinion on Drug Discovery, 4 (2009) 823-836.
[8] S.C. Gupta, C. Sundaram, S. Reuter, B.B. Aggarwal, Inhibiting NF-κB activation by small molecules as a therapeutic strategy, Biochimica et Biophysica Acta (BBA) - Gene Regulatory Mechanisms, 1799 (2010) 775-787.
[9] M. Karin, Y. Yamamoto, Q.M. Wang, The IKK NF-[kappa]B system: a treasure trove for drug development, Nat Rev Drug Discov, 3 (2004) 17-26.
[10] J.K. Durand, A.S. Baldwin, Targeting IKK and NF-κB for Therapy, Advances in Protein Chemistry and Structural Biology, 107 (2017) 77-115.
[11] T.D. Gilmore, M. Herscovitch, Inhibitors of NF-kappaB signaling: 785 and counting, Oncogene, 25 (2006) 6887-6899.
[12] J.A. Schmid, A. Birbach, IκB kinase β (IKKβ/IKK2/IKBKB)—A key molecule in signaling to the transcription factor NF-κB, Cytokine & growth factor reviews, 19 (2008) 157-165.
[13] C. Gamble, K. McIntosh, R. Scott, K.H. Ho, R. Plevin, A. Paul, Inhibitory kappa B kinases as targets for pharmacological regulation, British Journal of Pharmacology, 165 (2012) 802-819.
[14] A. Oeckinghaus, M.S. Hayden, S. Ghosh, Crosstalk in NF-[kappa]B signaling pathways, Nat Immunol, 12 (2011) 695-708.
[15] M. Hinz, C. Scheidereit, The IκB kinase complex in NF-κB regulation and beyond, EMBO reports, 15 (2014) 46-61.
[16] J.J. Huang, H.X. Chu, Z.Y. Jiang, X.J. Zhang, H.P. Sun, Q.D. You, Recent advances in the structure-based and ligand-based design of IKKbeta inhibitors as anti-inflammation and anti-cancer agents, Current medicinal chemistry, 21 (2014) 3893-3917.
[17] T. Dong, C. Li, X. Wang, L. Dian, X. Zhang, L. Li, S. Chen, R. Cao, L. Li, N. Huang, S. He, X. Lei, Ainsliadimer A selectively inhibits IKKα/β by covalently binding a conserved cysteine, 6 (2015) 6522.
[18] H. Park, Y. Shin, H. Choe, S. Hong, Computational Design and Discovery of Nanomolar Inhibitors of IκB Kinase β, Journal of the American Chemical Society, 137 (2015) 337-348.
[19] S. Saxena, G. Samala, J.P. Sridevi, P.B. Devi, P. Yogeeswari, D. Sriram, Design and development

of novel Mycobacterium tuberculosis L-alanine dehydrogenase inhibitors, European journal of medicinal chemistry, 92 (2015) 401-414.

[20] I.B. Levshin, I.V. Grigor'eva, A.A. Tsurkan, K.A. V'Yunov, A.I. Ginak, Study of azolidine reactivity and tautomerism. 53. Synthesis of 5-arylidene-2-(allylamino)-Δ2-thiazolin-4-ones and 5-arylidene-2-imino-3-allylthiazolidin-4-ones, Khim. Geterotsikl. Soedin., (1985) 494-497.

[21] S.Q. Tang, Y.Y.I. Lee, D.S. Packiaraj, H.K. Ho, C.L.L. Chai, Systematic Evaluation of the Metabolism and Toxicity of Thiazolidinone and Imidazolidinone Heterocycles, Chem. Res. Toxicol., 28 (2015) 2019-2033.

[22] J. Yong, M.Q. Christopher, K. Silvia, V.T. Robert, Current In Vitro Kinase Assay Technologies: The Quest for a Universal Format, Current Drug Discovery Technologies, 5 (2008) 59-69.

[23] S. Gul, P. Gribbon, Exemplification of the challenges associated with utilising fluorescence intensity based assays in discovery, Expert Opinion on Drug Discovery, 5 (2010) 681-690.

[24] R.S. Obach, R.L. Walsky, K. Venkatakrishnan, Mechanism-based inactivation of human cytochrome p450 enzymes and the prediction of drug-drug interactions, Drug metabolism and disposition: the biological fate of chemicals, 35 (2007) 246-255.

[25] M. Reynoso, A. Geddis, A. Mitrophanov, J. Ronald W Matheny, S. Hobbs, NFkB activation and cytokine output in LPS-treated RAW 264.7 macrophages, The FASEB Journal, 31 (2017) lb146-lb146.

[26] K.-J. Yun, J.-Y. Kim, J.-B. Kim, K.-W. Lee, S.-Y. Jeong, H.-J. Park, H.-J. Jung, Y.-W. Cho, K. Yun, K.-T. Lee, Inhibition of LPS-induced NO and PGE2 production by asiatic acid via NF-κB inactivation in RAW 264.7 macrophages: Possible involvement of the IKK and MAPK pathways, International Immunopharmacology, 8 (2008) 431-441.

[27] Z. Yan, P.P. Stapleton, T.A. Freeman, M. Fuortes, J.M. Daly, Enhanced expression of cyclooxygenase-2 and prostaglandin E2 in response to endotoxin after trauma is dependent on MAPK and NF-kappaB mechanisms, Cellular immunology, 232 (2004) 116-126.

[28] N. Futaki, S. Takahashi, M. Yokoyama, I. Arai, S. Higuchi, S. Otomo, NS-398, a new anti-inflammatory agent, selectively inhibits prostaglandin G/H synthase/cyclooxygenase (COX-2) activity in vitro, Prostaglandins, 47 (1994) 55-59.

[29] T. van der Bruggen, S. Nijenhuis, E. van Raaij, J. Verhoef, B. Sweder van Asbeck, Lipopolysaccharide-Induced Tumor Necrosis Factor Alpha Production by Human Monocytes Involves the Raf-1/MEK1-MEK2/ERK1-ERK2 Pathway, Infection and Immunity, 67 (1999) 3824-3829.

[30] L. Shi, R. Kishore, M.R. McMullen, L.E. Nagy, Lipopolysaccharide stimulation of ERK1/2 increases TNF-alpha production via Egr-1, American journal of physiology. Cell physiology, 282 (2002) C1205-1211.

[31] B.T. Priest, I.M. Bell, M.L. Garcia, Role of hERG potassium channel assays in drug development, Channels (Austin, Tex.), 2 (2008) 87-93.

[32] J.N. Singh, S.S. Sharma, hERG Potassium Channels in Drug Discovery and Development, in: S.P. Gupta (Ed.) Ion Channels and Their Inhibitors, Springer Berlin Heidelberg, Berlin, Heidelberg, 2011, pp. 149-190.

[33] M.C. Sanguinetti, M. Tristani-Firouzi, hERG potassium channels and cardiac arrhythmia, Nature,

440 (2006) 463-469.

[34] T. Danker, C. Möller, Early identification of hERG liability in drug discovery programs by automated patch clamp, Frontiers in Pharmacology, 5 (2014) 203.

Highlights

- Twenty four thiazolidinedione-scaffold based have been synthesized.
- Compounds **6v**, **6w**, and **6x** elicited IC_{50} values = 0.4, 0.7 and 0.9 µM respectively.
- Kinetic study of compounds **6v** and **6w** confirmed this class of modulators as irreversible inhibitors.
- LPS-treated RAW 264.7 macrophages proved the anti-inflammatory activity of compounds **6q** and **6v**.